Polymer Chemistry

ROYAL SOCIETY OF CHEMISTRY

REVIEW

View Article Online
View Journal

Cite this: DOI: 10.1039/d5py01177a

Strategies and chemistries for designing poly (ethylene oxide)-based solid-state electrolytes

Taohedul Islam and Xiangbo Meng *

Poly(ethylene oxide)-based solid polymer electrolytes (PEO-SPEs) are among the most extensively studied candidates for next-generation solid-state lithium batteries due to their favorable ion coordination, processability, and cost-effectiveness. However, their practical utilization is hindered by low room temperature conductivity, limited electrochemical stability, and vulnerability to dendrite formation. This review provides a comprehensive overview of recent advances in PEO-SPEs, focusing on polymer design strategies—including block copolymers, graft copolymers, crosslinked networks, and composite architectures through integration of organic and inorganic fillers, as well as ionic liquids. Furthermore, emerging salt chemistries such as single-ion/dual-ion conducting matrix and dual-salt systems are evaluated, in addition to the flame retardant formulations of the PEO-SPEs. By integrating insights from molecular engineering, interfacial science, and electrochemical characterization, this review highlights the synergistic pathways toward multifunctional PEO-SPEs capable of meeting the demands of high-energy, safe, and flexible solid-state lithium batteries.

Received 12th December 2025,
Accepted 12th January 2026

DOI: 10.1039/d5py01177a

rsc.li/polymers

The inception of research into poly(ethylene oxide) (PEO)-based solid-polymer electrolytes (SPEs) can be traced back to the 1970s,[1,2] notably preceding the emergence and commercialization of lithium-ion batteries.[3–5] Replacing flammable organic liquid electrolytes (oLEs) with solid-state electrolytes (SSEs) mitigates leakage and thermal runaway risks and enables direct use of lithium metal anodes (LMAs), which can substantially increase cell specific energy; however, realizing practical all solid state cells requires simultaneous optimization of ionic conductivity, electrochemical stability, mechanical robustness, and interfacial compatibility.[6–9] SSEs can broadly be categorized into inorganic ceramics and polymeric

Department of Mechanical Engineering, University of Arkansas at Fayetteville, Fayetteville, AR, USA. E-mail: xbmeng@uark.edu

Taohedul Islam

Dr Taohedul Islam is a Postdoctoral Research Fellow in Mechanical Engineering at the University of Arkansas, where he works on advanced solid polymer electrolytes for all-solid-state batteries under the supervision of Dr Xiangbo Meng. He received his Ph.D. in Chemistry from Jackson State University (Jackson, MS) in September 2022 and has been pursuing postdoctoral research since October 2022. His expertise spans material synthesis and atomic-scale characterization using synchrotron-based techniques, with a broader interest in structure–property relationships in complex systems.

Xiangbo Meng

Dr Xiangbo (Henry) Meng is an Associate Professor of Mechanical Engineering at the University of Arkansas (Fayetteville, AR). He holds two Ph.D. degrees: one in Mechanical & Materials Engineering (2011) and another in Chemical & Biochemical Engineering (2008), both from the University of Western Ontario (London, ON), Canada. He did his postdoctoral research at Argonne (Lemont, IL) and Brookhaven (Upton, NY) National Laboratories, USA, from 2011 to 2016. Since he joined the University of Arkansas in 2016, he has been directing a research group conducting studies on rechargeable batteries including lithium-ion batteries, lithium metal batteries, sodium batteries, and solid-state batteries.

systems, each offering distinct advantages and limitations. Inorganic electrolytes, such as oxides and sulfides, are valued for their high ionic conductivity and mechanical robustness, yet they often suffer from brittle fracture, difficult synthesis processes and poor interfacial compatibility with electrodes. In contrast, polyethylene oxide (PEO)-based polymer electrolytes provide flexibility, ease of processing, and better electrode contact, which draws more interest from the scientific community towards PEO-based SPEs for the applications in all-solid-state batteries using metal anodes. To highlight these complementary attributes, the following Table 1 summarizes the key differences between inorganic and PEO-based solid electrolytes.

PEO is a semi crystalline polyether whose repeating $–CH_2–O–CH_2–$ units provide ether oxygen lone pairs that coordinate Li^+ and promote salt dissociation, creating mobile charge carriers when salts such as lithium bis(trifluoromethanesulfonyl) imide (LiTFSI), lithium bis(fluorosulfonyl)imide (LiFSI), or $LiClO_4$ are dissolved into the polymer matrix.[10–13] Ion transport in PEO-based polymer electrolytes is governed by segmental motion of the polymer backbone and is therefore strongly coupled to the amorphous dynamics of the polymer;[14,15] the ionic conductivity scales with the fraction of amorphous phase and the rate of local chain relaxations, which in turn depend on molecular weight, salt concentration, and temperature.[15–17] At practical salt loadings and at ambient temperature, crystalline domains persist and confine fast transport to the amorphous regions, producing room temperature conductivities typically many orders of magnitude below those of oLEs unless additional design strategies are introduced.[18,19]

Three interrelated limitations constrain neat PEO electrolytes for room temperature operation. Firstly, pronounced crystallinity below ~60 °C that reduces the amorphous volume available for ion transport and lowers ionic conductivity to $\sim10^{-7}$ to 10^{-6} S cm^{-1} in many formulations.[20–22] Secondly, limited oxidative stability against high voltage cathodes often below ~4.0 V *versus* Li^+/Li depending on salt and additives.[23–25] Finally, mechanical weakness and poor resistance to lithium dendrite penetration under practical current densities, which undermines long term cycling with lithium metal anodes.[26] These intrinsic and interfacial shortcomings explain why unmodified single component PEO rarely meets the combined conductivity, stability, and mechanical criteria required for commercial solid-state batteries.

A diverse toolbox of materials strategies has emerged to decouple ionic transport from undesirable crystallinity while enhancing mechanical strength and electrochemical stability. One of the most widely used approaches is the incorporation of passive ceramic fillers (*e.g.*, Al_2O_3, SiO_2) to disrupt PEO crystallites, immobilize anions, and increase modulus.[27,28] Addition of ionically conductive inorganic fillers (garnets such as lithium lanthanum zirconium oxide, *i.e.*, LLZO, sodium super ionic conductor, *i.e.*, NASICON, or lithium aluminum titanium phosphate, *i.e.*, LATP) to provide parallel percolating Li^+ pathways are also proved to improve mechanical resistance to dendrite growth.[29,30] Plasticization of PEO to lower the glass-transition temperature (T_g), increase amorphous fraction, and enhance ambient-temperature conductivity has also been reported.[31,32] Synergistic combinations of these tactics have produced PEO-based composite electrolytes with substantially improved ambient temperature conductivity, extended electrochemical windows, and enhanced cycling stability in prototype cells.

Given the growing demand for safe, high-performance solid-state batteries, a comprehensive understanding of polymer design strategies for PEO-based electrolytes is both timely and essential. Despite decades of research, the ionic conductivity, mechanical robustness, and thermal stability of PEO systems remain interdependent challenges that require nuanced molecular engineering. Although previously published literature have discussed the performance and modification strategies of PEO-based solid polymer electrolytes, they often provide only a cursory overview of the underlying synthetic methodologies. In contrast, the present review is

Table 1 Differences in properties between inorganic and PEO-based solid electrolytes

Properties	Inorganic SSEs	PEO-based SPEs
Ionic conductivity	High (10^{-3}–10^{-2} S cm^{-1} at room temp for sulfides); often superior to polymers	Moderate (10^{-5}–10^{-3} S cm^{-1}); conductivity limited by PEO crystallinity and segmental motion
Li^+ transference number	Typically high (>0.5), depending on phase purity and defect chemistry	Lower (≈0.2–0.4), due to coupled ion–polymer segmental motion
Mechanical properties	Brittle and rigid; prone to fracture under stress	Flexible and processable; can form thin films and conformal coatings
Thermal stability	Excellent; stable up to 300–500 °C depending on chemistry	Moderate; stability improved with crosslinking or flame-retardant additives
Electrochemical stability window	Wide (up to 5–6 V *vs.* Li/Li^+ for oxides); for sulfides narrower (~2.5–3 V)	Narrower than inorganic ones(≈4–4.5 V *vs.* Li/Li^+); improved with salt/monomer design
Interfacial compatibility	Often poor with Li metal (dendrite penetration, high resistance); requires coatings or buffer layers	Better wetting and intimate contact with electrodes; but prone to instability at high current densities
Crystallinity effects	Inorganic phases are crystalline or glassy; ion transport *via* defect pathways	PEO crystallinity suppresses ion mobility; amorphization strategies (crosslinking, fillers) improve performance
Processability	Difficult; requires high-temperature sintering or complex densification	Easy; solution casting, melt processing, and scalable polymerization routes
Safety considerations	Nonflammable, but brittle fracture can cause short circuits; sulfides may release toxic gases	Safer mechanically (flexible, less brittle), but flammability risk unless modified

uniquely centered on the chemistry of synthesis, offering a detailed account of diverse polymerization techniques. By systematically analyzing how each synthetic route influences molecular architecture, crystallinity, and ion transport, this article provides a depth of coverage not found in existing literature. This review aims to consolidate and critically evaluate recent advances in the synthesis and structural tailoring of PEO, with a particular focus on strategies that enhance ion transport and safety. Following this introductory part, readers can expect an in-depth discussion of polymer architectures including block copolymers, graft copolymers, crosslinked networks, and composite systems, as well as complementary approaches such as lithium salt design and flame-retardant formulations, as illustrated in Fig. 1. Because the central aim of this review is to provide a synthesis-focused perspective, we deliberately did not include detailed battery performance data. Our emphasis is on polymerization methodologies and how different synthetic routes shape the molecular architecture and ion transport properties of PEO-based electrolytes. While electrochemical performance metrics are important, they have been extensively covered in prior reviews; by contrast, our contribution lies in offering a comprehensive and systematic account of synthesis strategies, which has not been addressed in comparable depth elsewhere. By mapping these diverse strategies onto performance metrics and practical considerations, this review seeks to guide future innovations in SPE development.

1. Block copolymers

Block copolymers are polymers made by linking two or more distinct polymer chains (blocks) together in a single macromolecule. Each block has different chemical or physical properties, which allows the material to self-assemble into well-defined nanostructures such as lamellae, cylinders, or spheres. In SPEs, block copolymers are especially useful because one block can facilitate ion transport (*e.g.*, PEO), while the others provide mechanical strength or thermal stability. Recent developments in PEO-based block copolymer architectures have showcased a wide array of molecular design strategies aimed at enhancing ion transport, segmental mobility, and structural tunability—core attributes for high-performance SPEs. Campos-Villalobos *et al.* used coarse-grained molecular dynamics simulations to explore the solvent-driven self-assembly of poly(ethylene oxide)-*b*-poly(butyl methacrylate) (PEO-*b*-PBMA) block copolymers in tetrahydrofuran (THF)/water mixtures.[33] They mapped a detailed morphological phase diagram for two copolymers (PEO6-*b*-PBMA4 and PEO12-*b*-PBMA10), revealing a rich variety of mesophases—including clusters, sheets, rod-like and spherical vesicles, lamellae, and kinetically trapped spheres—depending on the copolymer concentration and solvent composition (Fig. 2A). The study showed that increasing water content (selective for PEO) drives transitions from disordered clusters to more ordered structures like vesicles and lamellae, due to enhanced segregation between hydrophilic and hydrophobic blocks. Notably, the critical water content for micellization (~50 wt%) aligned with experimental observations. The simulations also revealed solvent redistribution around aggregates, with THF preferentially associating with PEO, influencing internal vesicle structure.

Building on the theme of block copolymer self-assembly, Daubian *et al.* introduced a one-pot microwave-assisted synthesis of asymmetric ABC triblock copolymers, specifically PEO-*b*-PEHOx-*b*-PEtOz, using sequential cationic ring-opening polymerization.[34] Their design enables directional self-assembly into asymmetric polymersomes (Fig. 2E), where curvature-driven segregation places the longer PEO block on the outer leaflet and the shorter PEtOz block on the inner. This architec-

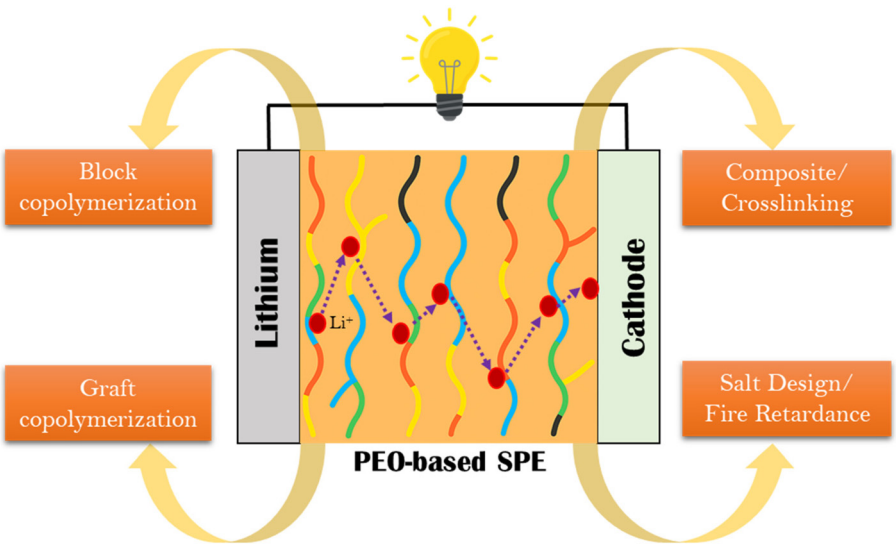

Fig. 1 Schematic representation of the utilization of PEO-based SPE and the different routes of SPE modifications.

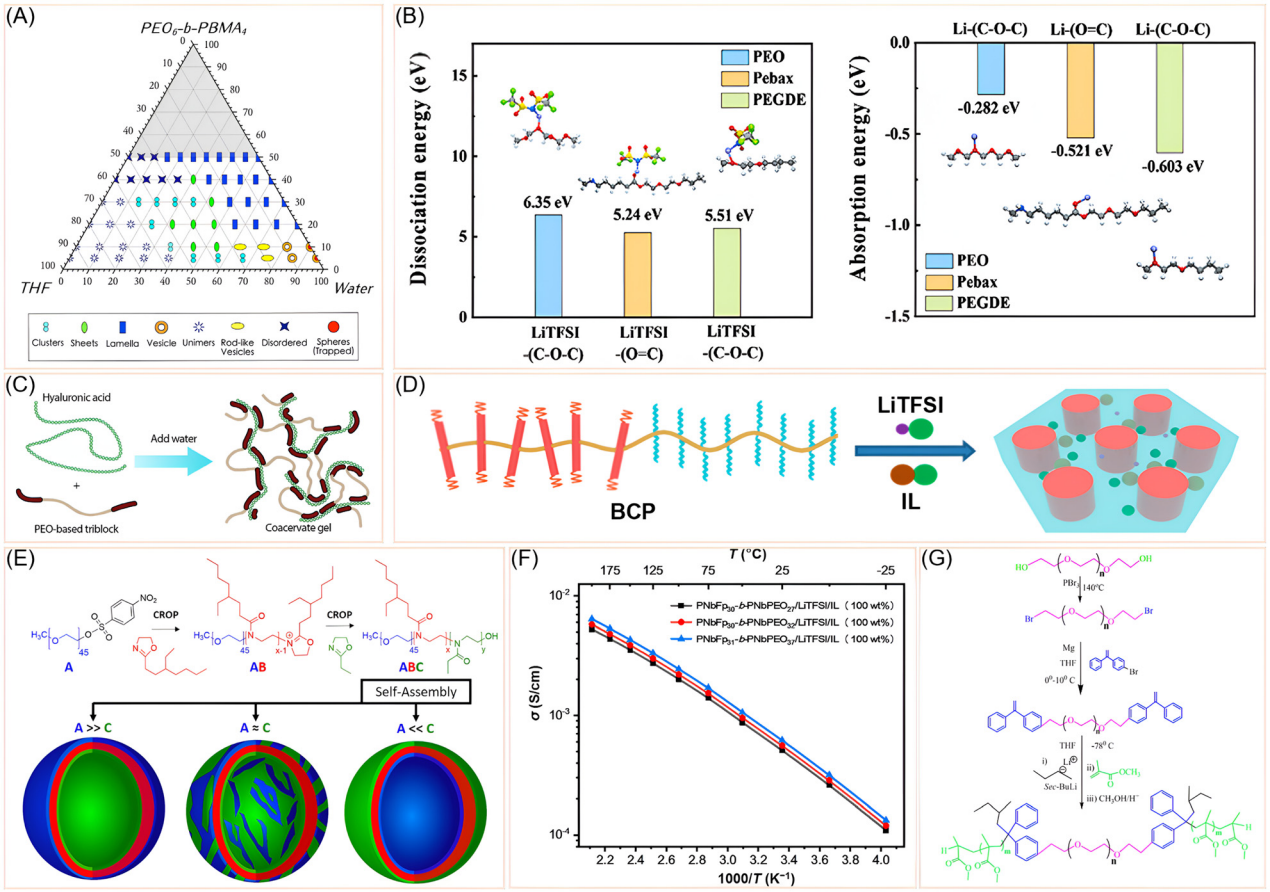

Fig. 2 (A) Morphological diagram of PEO_6-*b*-$PBMA_4$ in water and THF at 300 K. Reprinted with permission from ref. 33. Copyright (2020) Elsevier. (B) Calculated dissociation energy of LiTFSI to Li^+, $TFSI^-$ and Li^+ adsorption energy for PEO, Pebax, and PEGDE. Reprinted with permission from ref. 40. Copyright (2022) Elsevier. (C) Coacervate hydrogels by dissolving hyaluronic acid and the PEO-based triblock copolymer in water. Reprinted with permission from ref. 35 under a Creative Commons Attribution (CC BY-NC) License 4.0. (D) Schematic illustration of the self-assembling behavior of $PNbFp_{31}$-*b*-PNbPEO $_{37}$/LiTFSI/IL. Reprinted with permission from ref. 36 under a Creative Commons Attribution (CC BY-NC) License 4.0. (E) Synthesis scheme of PEO-*b*-PEHOx-*b*-PEtOz and the possible membrane orientations. Reprinted with permission from ref. 34. Copyright (2020) American Chemical Society. (F) σ values of the BCP/LiTFSI/IL complexes with 100 wt% of IL. Reprinted with permission from ref. 36 under a Creative Commons Attribution (CC BY-NC) License 4.0 (G) Synthesis scheme of PMMA-*b*-PEO-*b*-PMMA tri-block copolymers. Reprinted with permission from ref. 44. Copyright (2024) Taylor and Francis Group.

tural asymmetry, confirmed *via* bicinchoninic acid assay and 2D-NOESY NMR, offers a novel route to spatially controlled nanostructures, potentially adaptable for ion-selective transport in SPEs. In a complementary direction, Mabesoone *et al.* developed biohybrid hydrogels *via* ionic coacervation between hyaluronic acid (HA) and synthetic X-PEO-X triblock copolymers,[35] where X represents ammonium or guanidinium-functionalized blocks. Their design leverages noncovalent ionic interactions to form self-healing hydrogels with independently tunable mechanical stiffness and water content (Fig. 2C). By systematically varying the length and chemistry of the ionic end-blocks and the central PEO segment, they demonstrated how block architecture governs viscoelasticity and charge balance, offering a modular framework translatable to SPEs.

Shifting focus to synthetic methodology, Li *et al.* developed a ligand-free iron-mediated ATRP (Atom Transfer Radical Polymerization) system using Br-terminated PEO (PEO-Br) as both initiator and coordinating ligand.[37] This green synthetic route enabled the formation of PEO-*b*-PMMA (PMMA: poly methyl methacrylate) and PEO-*b*-PEGMA (PEGMA: poly (ethylene glycol) mono methacrylate) block copolymers with tunable EO content and molecular weight. Their study revealed that longer PEO chains enhance coordination with $FeBr_2$, improving polymerization control and ultimately ionic conductivity in P(EO-PEGMA)/PVDF composite electrolytes. This dual-functionality of PEO-Br as initiator and ligand offers a scalable and environmentally benign pathway to SPE-relevant architectures. To address the persistent challenge of PEO crystallinity, Wu *et al.* synthesized a series of polynorbornene-based block copolymers (BCPs) *via* tandem ring-opening metathesis polymerization (ROMP), incorporating short PEO side chains and rigid liquid crystalline (LC) side chains.[36] These BCPs were designed to suppress PEO crystallization and enhance mechanical and thermal stability. The molecular architecture was tailored by

adjusting the degree of polymerization of each block, yielding well-defined lamellar (LAM) or hexagonally packed cylindrical (HEX) nanostructures upon doping with LiTFSI and ionic liquid (EMIMTFSI: 1-ethyl-3-methylimidazolium trifluoromethanesulfonate) (Fig. 2D). SAXS analysis confirmed the formation and thermal persistence of these nanostructures up to 200 °C, attributed to the LC behavior of the rigid side chains. The PEO domains served as ion-conducting channels, while the rigid domains provided mechanical integrity. The incorporation of IL enhanced ionic conductivity (Fig. 2F) and facilitated microphase separation. Rheological measurements showed that the electrolytes maintained solid-like behavior across a wide temperature range, with storage moduli (G') exceeding loss moduli (G'') up to 200 °C. This dual-phase design strategy enabled the development of BCP electrolytes with suppressed crystallinity, high ionic conductivity, and robust thermal and mechanical properties. In another strategy aimed at enhancing amorphous character and segmental mobility, Kunitskaya *et al.* explored triblock copolymers of PAAm-*b*-PEO-*b*-PAAm and their hydrolyzed derivatives, forming intramolecular polycomplexes (IntraPCs) *via* hydrogen bonding.[38] This design suppresses PEO crystallinity and enhances amorphous character, thereby improving segmental mobility and ionic conductivity. Their work demonstrates that increasing PEO block length and introducing carboxylic acid groups into the PAAm segments synergistically enhance conductivity, especially when doped with $LiPF_6$—an approach that combines hydrogen bonding and ionic functionalization within a block copolymer matrix.

Delving into interfacial phenomena, Sharon *et al.* provided molecular-level insights into ion solvation and distribution in SEO-LiTFSI block copolymer electrolytes (polystyrene-*block*-PEO is abbreviated as SEO) compared to PEO homopolymers.[39] Using vibrational spectroscopy and atomistic simulations, they revealed that SEO maintains optimal conductivity at higher salt concentrations due to ion segregation at PS/PEO interfaces (PS = polystyrene). This interfacial localization preserves free solvation sites within the PEO domains, a phenomenon absent in homopolymers. Their findings underscore how block copolymer morphology and interfacial chemistry can be engineered to decouple conductivity loss from salt loading—a critical consideration in SPE formulation. Further advancing the design of mechanically robust and conductive systems, Yang *et al.* reported a plasticizer-free block copolymer with conductive nanodomain, using poly(ether-*block*-amide) (Pebax) as the principal matrix including polyethylene glycol dimethyl ether (PEGDE) as a regulator, which connects the Li^+ transport channels.[40] Density functional theory (DFT) calculation reveals that LiTFSI dissociation and Li^+ absorption is much easier in Pebax and PEGDE compared to PEO (Fig. 2B). A combination of Pebax and nanodomain connector PEGDE altogether contributes to an ionic conductivity of 4.47×10^{-4} S cm^{-1} at 60 °C. The P–P electrolyte (Pebax-PEGDE) shows its ultimate strength when utilized in a Li||Li symmetric cell, showing stable lithium plating/stripping behaviors over 2000 hours. In an all-solid-state assembly, the P–P electrolyte with $LiFePO_4$ (LFP) cathode and LMA demonstrates ultra-long cycle life at 0.5 C (1 C = 0.68 mA cm^{-2}), accounting for 1300 cycles with a capacity retention of 82.8%. In parallel, Zhang *et al.* synthesized a block copolymer of the composition poly(ethylene oxide)-*b*-poly(trimethyl-*N*-((2-(dimethylamino)ethyl methacrylate)-7-propyl)-ammonium bis(trifluoromethane-sulfonyl)imide) (PEO-*b*-PDM-dTFSI), where the PDM-dTFSI block contains double quaternary ammonium cations and serves as a second ion-conductive phase alongside PEO.[41] Their work highlights the importance of dual-phase conduction and ordered lamellar morphologies in achieving both high ionic conductivity and mechanical robustness. By tuning the salt doping ratio and block composition, they achieved phase-separated structures that facilitate ion transport while suppressing lithium dendrite formation—an architectural principle highly relevant to SPE design.

To further expand the structural diversity of PEO-based block copolymers, Masud *et al.* synthesized a series of triblock copolymers with the architecture PAN-*b*-PEO-*b*-PAN using reversible addition–fragmentation chain transfer (RAFT) polymerization, employing a bifunctional PEG-based macro chain transfer agent.[42] These block copolymers combine the mechanical strength and dipole-rich nitrile groups of polyacrylonitrile (PAN) with the high dielectric constant and chain flexibility of poly(ethylene oxide) (PEO), making them structurally promising for ion-conductive systems. The RAFT-synthesized polymers initially contained trithiocarbonate end groups, which were systematically modified using two effective strategies: lauroyl peroxide (LPO) radical-induced cleavage and a bromination route involving *N*-bromosuccinimide (NBS) and triphenylphosphine dibromide (PPh_5Br_2). These methods successfully removed the UV-absorbing and potentially reactive trithiocarbonate groups, yielding more stable end-functionalized polymers. Thermal analysis revealed that all PAN-based block copolymers were stable above 200 °C, with significant weight retention due to ladder-like cyclization of nitrile groups at elevated temperatures.

Exploring thermoresponsive behavior, Tripathi *et al.* investigated the salt-induced micellization of commercially available PEO-PPO-PEO triblock copolymers, specifically Pluronics L44 (PEO_{10}-PPO_{23}-PEO_{10}) and F77 (PEO_{53}-PPO_{34}-PEO_{53}), in aqueous environments.[43] These block copolymers exhibit thermoresponsive self-assembly, transitioning from molecularly dissolved unimers to organized micellar structures as temperature and concentration increase. L44, with lower PEO content and molecular weight, is moderately hydrophilic, while F77 is highly hydrophilic due to its higher PEO fraction. The study explored how sodium salts (NaCl and Na_2SO_4) influence micellization, cloud point (CP), and micelle morphology. Salt addition was found to modulate hydration and inter-block interactions, promoting earlier micellization and structural transitions from spherical to ellipsoidal micelles. Using techniques such as high-sensitivity differential scanning calorimetry (HSDSC), dynamic light scattering (DLS), and small-angle neutron scattering (SANS), the authors quantified changes in micelle size, shape, and aggregation behavior. In a related

effort to understand micelle formation and block architecture effects, Das *et al.* synthesized PMMA-*b*-PEO-*b*-PMMA triblock copolymers *via* living anionic polymerization using telechelic 1,1-diphenylethylene-terminated PEO macroinitiators (Fig. 2G).[44] Their design emphasizes the amphiphilic nature of the triblock, where PMMA forms the hydrophobic core and PEO the hydrophilic corona in flower-like micelles. By varying block lengths, they demonstrated how micelle size and dispersity are governed by the balance between hydrophobic and hydrophilic segments. Though focused on metal ion detection, their structural insights into micelle formation and block length effects are directly applicable to nanostructured SPEs, particularly in tailoring ion-conductive domains and optimizing interfacial transport.

Altogether, these studies underscore the remarkable versatility of block copolymer architectures in tailoring the structural, mechanical, and electrochemical properties of PEO-based solid polymer electrolytes. Through strategic manipulation of block composition, length, functionalization, and self-assembly behavior, researchers have demonstrated pathways to suppress crystallinity, enhance ion transport, and improve thermal and mechanical stability. Whether through hydrogen bonding, dual-phase conduction, curvature-driven segregation, or thermoresponsive micellization, the design principles emerging from these works offer a modular and scalable framework for next-generation SPEs. These insights lay a strong foundation for exploring other polymer design strategies—such as grafting, crosslinking, and composite formation—which further expand the functional landscape of PEO-based systems.

2. Graft copolymers

Recent advances in graft copolymer architecture have significantly expanded the design space for high-performance SPEs, particularly those based on PEO. A central challenge in PEO-based SPEs is their semi-crystalline nature at ambient temperatures, which restricts lithium-ion mobility and limits ionic conductivity. To address this, researchers have explored various grafting strategies—ranging from backbone-grafted brush copolymers to nanoparticle-grafted single-ion conductors (SICs)—that disrupt crystallinity, enhance segmental dynamics, and improve electrochemical stability. One compelling approach reported by Wu *et al.*, where they investigated the influence of side chains on the solution-phase self-assembly of polyphenylene-based "rod-coil" graft copolymers, specifically PPP-*g*-PEO and PPP-*g*-PAA.[45] These copolymers feature a rigid poly-*p*-phenylene (PPP) backbone grafted with flexible PEO or poly(acrylic acid) (PAA) coils. By systematically varying the grafting percentage (GP) and degree of polymerization (DP) of the side chains, they demonstrated that PPP-*g*-PEO exhibits temperature-dependent hierarchical self-assembly in THF-water mixtures. Above the crystallization temperature (T_c) of PEO, the copolymers formed ultralong helices or nanowires depending on the steric crowding parameter PVN, while below T_c, polygonal multilayer nanosheets emerged when PVN exceeded a critical threshold. PPP-*g*-PAA, on the other hand, showed pH-responsive behavior, forming diverse low-dimensional nanostructures as electrostatic repulsion among PAA coils varied.

Expanding the use of amphiphilic graft copolymers for ion transport, He *et al.* developed a novel strategy for fabricating polymer electrolyte membranes (PEMs) with continuous ion-conducting channels using polycyclooctene-*graft*-polyethylene glycol (PCOE-*g*-PEG).[46] By dialyzing the copolymer solution in a PEG-selective solvent (ethanol), self-assembled micelles with PEG shells and PCOE cores were formed (Fig. 3A), which upon thermal treatment fused into a bicontinuous morphology. This structure enabled the formation of mechanically robust PCOE domains and continuous PEG channels for lithium ion transport. Remarkably, even with just 20 wt% PEG (M_n = 350 g mol^{-1}), the self-assembled PEMs (S-PEMs) achieved room-temperature ionic conductivity exceeding 10^{-4} S cm^{-2}—2 to 3 orders of magnitude higher than that of the directly cast PEMs (D-PEMs) with the same composition. The S-PEMs also demonstrated superior electrochemical stability (~4.6 V), mechanical strength, and cycling performance in LFP‖Li cells, outperforming D-PEMs. In a related effort targeting flexible energy storage, Kang *et al.* introduced a novel graft copolymer electrolyte, PEGBEM-*g*-PAEMA, designed for solid-state bendable supercapacitors.[47] Synthesized *via* free-radical polymerization, this copolymer combines ethylene oxide-rich PEGBEM (poly(ethylene glycol) behenyl ether methacrylate) for polarity and mechanical strength with amorphous PAEMA (poly(2-acetoacetoxy)ethyl methacrylate) segments that enhance ionic conductivity (Fig. 3B). When blended with the ionic liquid (IL) $EMIMBF_4$ (1-ethyl-3-methylimidazolium tetrafluoroborate), the resulting electrolyte formed a flexible, leak-free solid film up to 200% IL content. The optimized electrolyte exhibited high ionic conductivity (1.23×10^{-3} S cm^{-1}), excellent thermal stability, and a wide electrochemical window.

To further explore nanostructured ion-conducting pathways, Ji *et al.* introduced a class of solid-state lithium-ion conductors based on mixed-graft block copolymers (mGBCPs) that integrate short PEO with polydimethylsiloxane (PDMS) side chains (Fig. 3D).[48] These mGBCPs were synthesized *via* ring-opening metathesis polymerization of norbornene-functionalized macromonomers, enabling nanophase separation even with low-molecular-weight side chains. Through tuning the PEO/PDMS volume fractions, they achieved diverse morphologies—such as double gyroids, hexagonally perforated lamellae, and cylinders—that facilitated continuous ion-conducting pathways. Importantly, blending mGBCPs with free amorphous PEO chains significantly enhanced Li^+ conductivity, reaching up to 2.0×10^{-4} S cm^{-1} at room temperature. This conductivity was achieved without compromising mechanical integrity, as the materials exhibited viscoelastic solid behavior with storage moduli in the 10^4–10^5 Pa range.

Incorporating degradability into graft copolymer design, Du *et al.* explored the radical ring-opening polymerization (rROP) of cyclic ketene acetals (CKAs), specifically 2-methylene-1,3,6-

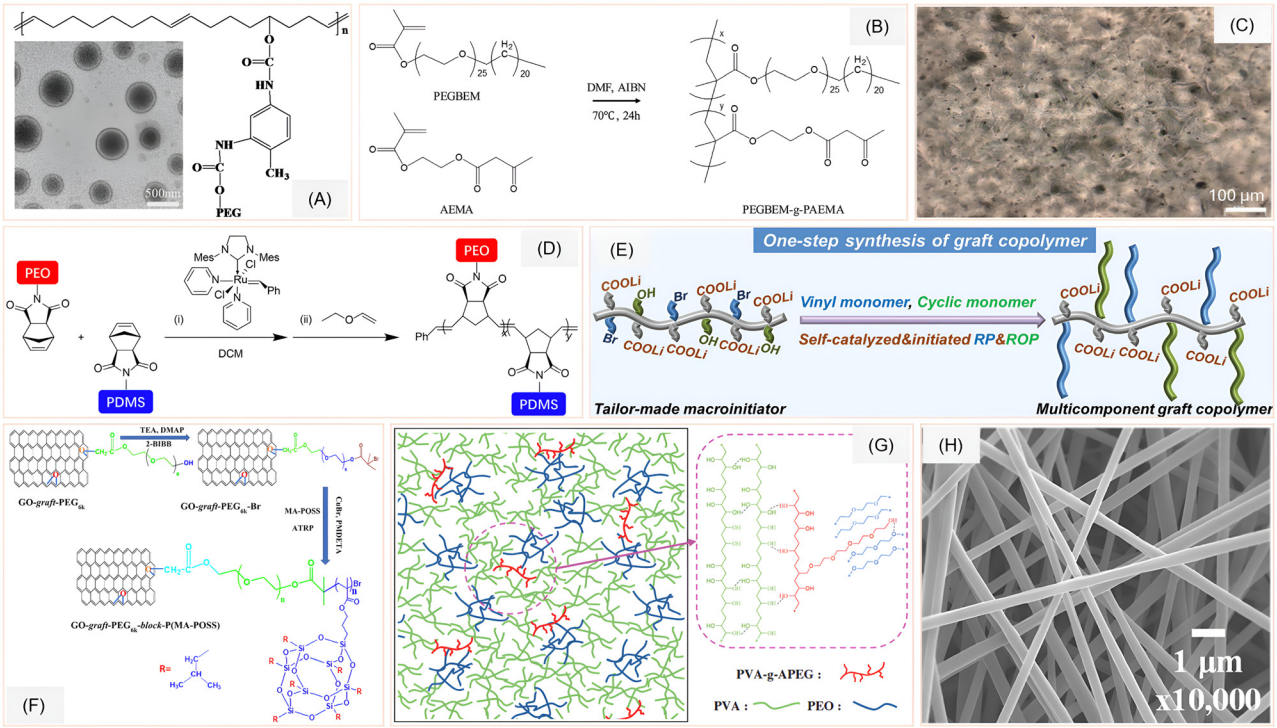

Fig. 3 (A) Structure of PCOE-*g*-PEG (inset: SEM of the self-assembled micelles). Reprinted with permission from ref. 46. Copyright (2019) Elsevier. (B) Structure of PEGBEM-*g*-PAEMA copolymer. Reprinted with permission from ref. 47. Copyright (2020) Elsevier. (C) POM images of 1%GO-*g*-PEG$_6$k-*b*-P(MA-POSS) nanocomposite solid polymer electrolyte. Reprinted with permission from ref. 52. Copyright (2023) American Chemical Society. (D) Synthesis scheme of mGBCPs. Reprinted with permission from ref. 48 under a Creative Commons Attribution (CC BY-NC-ND) License 4.0. (E) One-step synthesis of graft copolymer using self-catalyzed and self-initiated radical and ring opening polymerization. Reprinted with permission from ref. 50. Copyright (2023) John Wiley & Sons. (F) Synthesis scheme of GO-*g*-PEG$_6$k-*b*-P(MA-POSS). Reprinted with permission from ref. 52. Copyright (2023) American Chemical Society. (G) Local orientation of PVA-*g*-APEG copolymer networking between PVA/PEO strands. Reprinted with permission from ref. 51. Copyright (2022) John Wiley & Sons. (H) SEM image of PVA-*g*-APEG nanofibers. Reprinted with permission from ref. 51. Copyright (2022) John Wiley & Sons.

trioxocane (MTC) and 5,6-benzo-2-methylene-1,3-dioxepane (BMDO), to synthesize degradable polyesters and PEO-based graft copolymers.[49] Through detailed mechanistic studies, they demonstrated that both CKAs undergo 100% ring-opening, with BMDO forming stable benzyl radicals and MTC generating more reactive alkyl radicals prone to branching. By employing semi-batch copolymerization with *N*-vinyl pyrrolidone (NVP), they achieved uniform ester distribution and tunable copolymer architectures. Notably, they leveraged radical transfer to PEO in a PEO solvent system to graft CKA-*co*-NVP side chains onto PEO backbones, yielding degradable graft copolymers with controlled composition.

A one-step method that simultaneously combines radical polymerization (RP) and ring-opening polymerization (ROP) is introduced by Guo *et al.* using a lithium carboxylate-based macroinitiator (PAALi(OH-Br)).[50] This strategy enables the synthesis of graft copolymer electrolytes (GCPEs) with polystyrene (PS) backbones and side chains of poly(ethylene glycol) (PEG) and poly(ε-caprolactone) (PCL) (Fig. 3E). The brush-like topology not only suppresses PEO and PCL crystallization but also facilitates intra-chain lithium-ion hopping. The resulting $PS_{0.20}$-$PCL_{0.25}$-$PEG_{0.55}$ electrolyte demonstrated a balanced profile of mechanical robustness (1.62 MPa tensile stress), high ionic conductivity (2.4×10^{-5} S cm^{-1} at 30 °C), and a lithium-ion transference number (tLi$^+$) of 0.47. Notably, the electrochemical stability window extended to 4.8 V, making it compatible with high-voltage cathodes. Addressing morphological stability in blended systems, Yang *et al.* synthesized a novel compatibilizer, PVA-*g*-APEG, *via* free radical polymerization and alcoholysis, to stabilize PVA/PEO blends used for biomedical nanofiber membranes (PVA: polyvinyl alcohol; APEG: alcohol-allyl polyethylene glycol) (Fig. 3G).[51] The graft copolymer prevented phase separation over extended periods, enabling continuous electrospinning and producing nanofibers with uniform morphology (Fig. 3H). Although this work is more aligned with biomedical applications, the compatibilization strategy could be adapted to stabilize PEO-based blends in energy storage contexts, particularly where long-term morphological stability is essential.

Utilization of graphene oxide (GO) in the polymer matrix was explored by Khan *et al.*, as they have reported the synthesis of brush-like nanofillers by grafting PEG$_6$k and poly(methacrylate-functionalized POSS) onto GO (Fig. 3C and F).[52] These GO-*g*-PEG$_6$k-*block*-P(MA-POSS) nanofillers were incorporated into

PEO matrices to form nanocomposite SPEs. The hybrid fillers introduced both Lewis acid–base interactions and steric hindrance, which improved salt dissociation and created interfacial ion-conducting pathways. The optimized formulation achieved an ionic conductivity of 3.0×10^{-4} S cm^{-1} at 50 °C, outperforming both pristine GO and GO-*g*-PEG$_6$k systems. The POSS nanocages likely contributed to increased free volume and enhanced chain mobility at the filler–polymer interface, further facilitating lithium-ion transport. Furthermore, a distinct grafting strategy is introduced by Liu *et al.*, where the author reported a composite solid electrolyte (CSE) in which a single-ion conducting (SIC) polymer—poly(lithium (4-styrenesulfonyl)(phenylsulfonyl)imide), or PLiSSPSI—was grafted onto SiO_2 nanoparticles *via* a thiol-disulfide exchange reaction.[53] These PLiSSPSI-*g*-SiO_2 fillers were then dispersed into a PEO/LiTFSI matrix. The resulting CSEs with a formulation of 6 wt% filler exhibited remarkable electrochemical performance, achieving an ionic conductivity of 2.2×10^{-4} S cm^{-1} at 60 °C and a tLi$^+$ of 0.77. The high transference number is particularly significant, as it minimizes concentration polarization and suppresses lithium dendrite formation. The grafted nanoparticles also disrupted PEO crystallinity, as confirmed by XRD and DSC, thereby increasing the amorphous content and enhancing ion mobility.

Collectively, these studies demonstrate the remarkable adaptability of graft copolymer architectures in advancing PEO-based solid polymer electrolytes. By tuning backbone rigidity, side-chain chemistry, grafting density, and self-assembly behavior, researchers have engineered systems that exhibit enhanced ionic conductivity, mechanical robustness, electrochemical stability, and even degradability. Whether through brush-like topologies, nanofiller integration, bicontinuous morphologies, or compatibilization strategies, graft copolymers offer a modular platform for overcoming the intrinsic limitations of PEO. These insights provide a strong foundation for exploring crosslinked and composite polymer systems, where network formation and hybrid interfaces further expand the design space for high-performance SPEs.

3. Crosslinked polymers

Recent studies have demonstrated that UV-induced crosslinking is a powerful strategy to overcome the limitations of PEO-based SPEs, particularly their high crystallinity, low mechanical strength, and limited ionic conductivity at ambient temperature. Falco *et al.* explored the UV-induced cross-linking of PEO/LiTFSI systems using benzophenone as a type II photoinitiator.[54] Type II photoinitiators are a class of compounds that initiate polymerization through a bimolecular process. Unlike Type I initiators which break apart on their own, Type II photoinitiators require a second molecule, called a co-initiator, to generate the necessary free radicals. Falco *et al.* demonstrated that UV curing significantly reduces PEO crystallinity and enhances mechanical robustness, yielding a quasi-solid electrolyte with ionic conductivity exceeding 0.1 mS cm^{-1} and lithium-ion transference numbers above 0.5. Through a combination of XRD, DSC, MAS-NMR, and rheological analyses, they showed that the cross-linked matrix retains its amorphous character and mechanical integrity even after long-term storage and thermal stress. Importantly, their polymer electrolyte enabled stable cycling in LFP-based lithium-metal cells, confirming its suitability for practical applications.

Building on UV-curing strategies, Zhang *et al.* developed a flexible SPE by integrating PEO, tetraethylene glycol dimethacrylate (TEGDMA), and tetraglyme (TEGDME) through a UV-induced *in situ* dual-reaction process.[55] This method simultaneously initiated cross-linking between PEO and TEGDME and polymerization of TEGDMA into a rigid linear oligomer (PTEGDMA), forming a hybrid network. The resulting PTT-SPE exhibited a highly amorphous structure, as confirmed by XRD and DSC, with a significantly reduced glass transition temperature, indicating enhanced segmental mobility. FTIR analysis confirmed the complete conversion of TEGDMA and successful incorporation of all components. The cross-linked architecture suppressed PEO crystallinity and improved mechanical integrity, while maintaining flexibility and elasticity. These structural modifications enhanced ionic conductivity (2.7×10^{-4} S cm^{-1} at 24 °C) and a lithium-ion transference number of 0.56, making the PTT-SPE a promising candidate for room-temperature solid-state lithium batteries.

In a distinct approach using ring-opening metathesis polymerization (ROMP), Hossain *et al.* reported a series of cross-linked copolymer membranes by combining PEG/PPG and PDMS (polydimethylsiloxane) macromonomers.[56] Both macromonomers were end-functionalized with norbornene groups to enable efficient cross-linking and formation of an interlocked network structure (Fig. 4F). This design suppressed crystallinity, enhanced segmental mobility, and improved thermomechanical properties. The resulting membranes exhibited single T_g values (−53 to −62.5 °C) and melting points (11.6 to 23.3 °C), which decreased with increasing PDMS content, indicating enhanced chain flexibility and free volume. Thermal analysis showed decomposition temperatures above 360 °C, with PDMS-rich compositions reaching up to 486 °C. Mechanical testing revealed tensile strengths up to 11 MPa and Young's moduli exceeding 500 MPa, with elongation at break improving with PDMS incorporation. These copolymers retained the amorphous state at operating temperatures and demonstrated excellent solvent resistance, confirming their highly cross-linked nature.

Extending the ROMP-based strategy, Zuo *et al.* introduced a novel hybrid triblock polymer electrolyte (HTPE) system based on poly(ε-caprolactone)-*block*-poly(ethylene glycol)-*block*-poly(ε-caprolactone) (PCL-*b*-PEG-*b*-PCL) copolymers crosslinked *via* initiator-free thiol–ene photopolymerization with thiol-functionalized polyhedral oligomeric silsesquioxane (POSS-SH) (Fig. 4B).[57] The triblock architecture combines the flexibility and ion-coordinating ability of PEG with the mechanical reinforcement and ester-rich coordination sites of PCL. Methacryloyl-functionalized PCL-PEG-PCL macromolecular

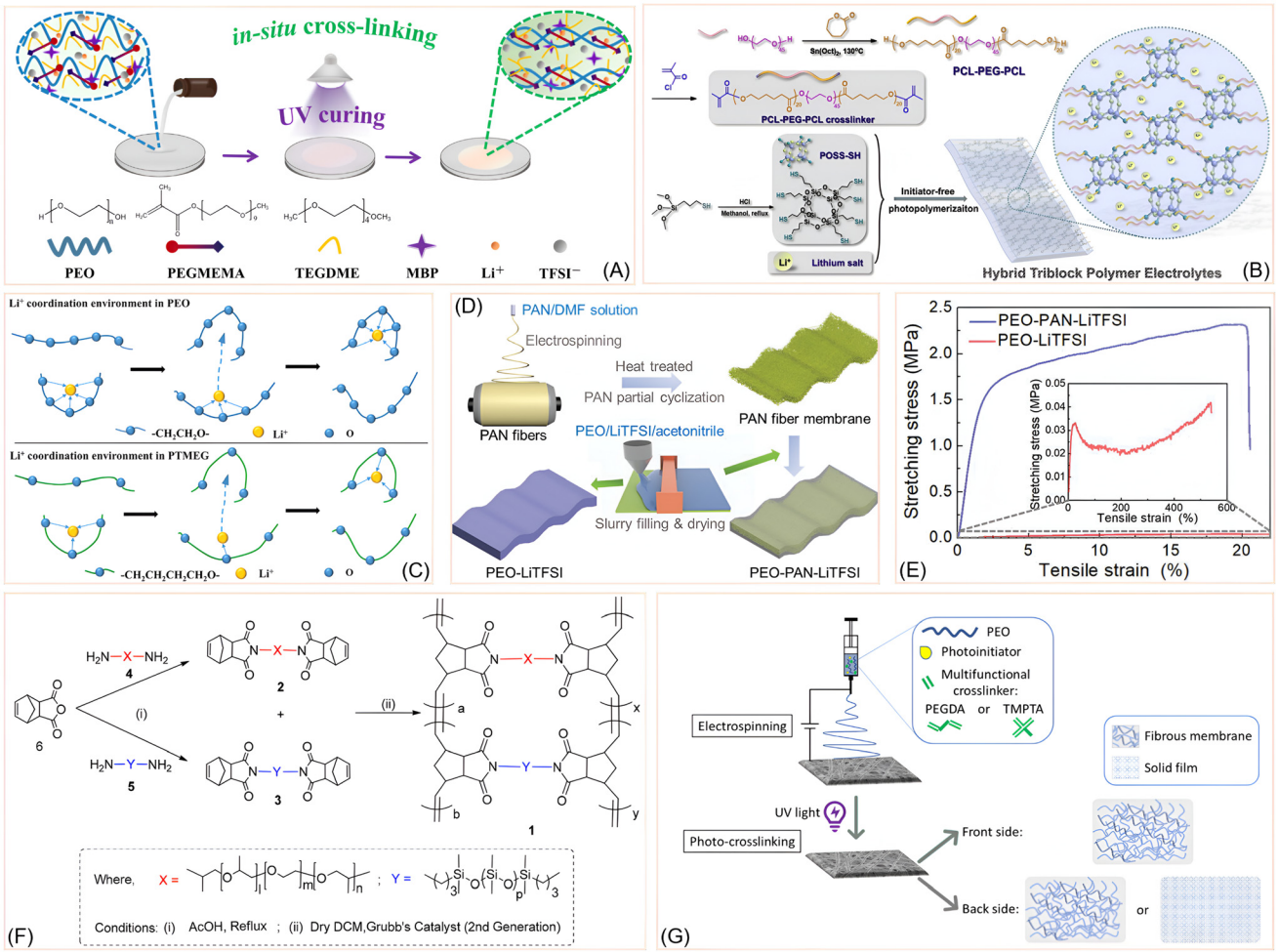

Fig. 4 (A) Schematic representation of *in situ* crosslinking initiated by UV-light. Reprinted with permission from ref. 62. Copyright (2023) Elsevier. (B) Illustration of PCL-PEG-PCL crosslinked polymer electrolyte. Reprinted with permission from ref. 57. Copyright (2020) Elsevier. (C) Li^+ coordination comparison in PEO and in PTMEG/VBIM-TFSI polymeric system. Reprinted with permission from ref. 58. Copyright (2021) Elsevier. (D) Preparation of PEO-PAN-LiTFSI membrane by electrospinning. Reprinted with permission from ref. 60. Copyright (2022) John Wiley & Sons. (E) Stress *vs.* strain curve for PEO and PEO-PAN matrices. Reprinted with permission from ref. 60. Copyright (2022) John Wiley & Sons. (F) Synthesis scheme of PEG/PPG:PDMS and its precursors. Reprinted with permission from ref. 56. Copyright (2020) American Chemical Society. (G) Illustration of the synthesis protocol of PEO-based crosslinked polymer by utilizing photo-initiator. Reprinted with permission from ref. 59 under a Creative Commons Attribution (CC BY) License 4.0.

crosslinkers were synthesized and reacted with POSS-SH under UV light to form a robust crosslinked network without requiring photoinitiators. Thermal analysis showed that increasing PCL content improved decomposition temperatures, with HTPE30 reaching 288 °C. DSC revealed decreasing glass transition temperatures (T_g from −24.3 to −37.1 °C) with higher PCL content, indicating enhanced segmental mobility. Mechanical testing demonstrated that HTPE20 achieved an optimal balance, with tensile strength of 9.57 MPa and strain up to 39%, outperforming PEGDMA-based controls. Electrochemical characterization showed that ionic conductivity increased with temperature and PCL content up to HTPE30, but declined in HTPE40 due to reduced PEG fraction. HTPE20 with 40% $LiClO_4$ achieved 6.41 × 10^{-3} S cm^{-1} at 100 °C. In a complementary direction, Dong *et al.* designed a series of freestanding crosslinked ionic copolymer electrolytes by UV-initiated copolymerization of vinyl-functionalized polytetramethylene ether glycol (vinyl-PTMEG) and polymerizable ionic liquid VBIM-TFSI. PTMEG was selected for its longer ether spacing (–$(CH_2)_4$–O–), which weakens Li^+ coordination compared to PEO and facilitates easier ion dissociation and transport (Fig. 4C).[58] VBIM-TFSI, a vinyl-imidazolium-based ionic liquid, was incorporated to provide mobile ionic species and enhance electrochemical stability. The resulting NPE membranes exhibited fully amorphous morphology, confirmed by XRD and FTIR, with suppressed crystallinity and uniform elemental distribution. Mechanical testing showed high tensile strength and elongation at break (up to 84%), while DSC revealed low glass transition temperatures ($T_g \approx$ −54 °C) and absence of melting peaks, indicating enhanced

segmental mobility. These structural features yielded improved ionic conductivity (~3.18×10^{-5} S cm^{-1}) and lithium-ion transference numbers (tLi$^+$ up to 0.47), making the PTMEG/VBIM-TFSI copolymer system a promising platform for ambient-temperature solid-state lithium batteries.

Electrospinning-based crosslinking strategies were also explored by Kianfar *et al.*, who focused on electrospun PEO membranes cross-linked with multifunctional acrylic monomers—PEGDA (polyethylene glycol diacrylate) and TMPTA (trimethylol propane triacrylate)—under UV irradiation (Fig. 4G).[59] Their study emphasized the role of cross-linker type and concentration in determining fiber morphology, porosity, and water resistance. TMPTA-based membranes exhibited superior uniformity and retained fibrous structure on both sides, while PEGDA systems showed partial film formation due to cross-linker migration. In a related electrospun system, Sheng *et al.* introduced a nanofiber-reinforced PEO-PAN (polyacrylonitrile) copolymer membrane (Fig. 4D) for lithium–sulfur (Li–S) batteries.[60] By electrospinning PAN fibers and cross-linking them with PEO chains, they achieved a mechanically robust (Fig. 4E), flexible, and ion-conductive membrane. The presence of C═N–O functional groups enabled polysulfide adsorption, effectively suppressing shuttle effects and improving cycling stability.

Further advancing UV-curable systems, Fu *et al.* developed a dual-salt PEO-based polymer electrolyte incorporating LiTFSI and LiODFB (lithium difluoro(oxalato)borate), cross-linked with tetraethylene glycol dimethyl ether (TEGDME) under UV irradiation.[61] The *in situ* polymerization approach yielded ultrathin membranes (~20 μm) with high ionic conductivity (0.57 mS cm^{-1} at 30 °C), a lithium-ion transference number of 0.79, and electrochemical stability up to 4.8 V. The formation of a LiF-rich cathode electrolyte interphase (CEI) layer on NCM622 cathodes suppressed PEO decomposition and enabled high-voltage cycling with 94.7% capacity retention after 100 cycles. To further enhance mechanical and electrochemical performance, Ji *et al.* designed a PEO-based SPE with a double crosslinked network structure.[62] The system integrates soft ether-based chains from PEO, tetraglyme (TEGDME), and polyethylene glycol methyl ether methacrylate (PEGMEMA), which undergo UV-induced crosslinking and polymerization (Fig. 4A). This dual mechanism forms a dense, amorphous matrix with suppressed crystallinity. The resulting SPE, termed PTP-SPE, exhibits a low glass transition temperature (T_g = −77 °C) and a reduced melting point (T_m = 31 °C), indicating enhanced segmental mobility. The mechanical properties were significantly improved, with tensile elongation reaching 40%, outperforming pristine PEO-SPE. Electrochemical characterization showed an ionic conductivity of 0.2 mS cm^{-1} and a lithium-ion transference number of 0.51 at room temperature, attributed to the amorphous structure and coordinated ester groups. To elucidate the relationship between ionic conductivity and mechanical properties, Naboulsi *et al.* investigated cross-linked PEO networks *via* radical copolymerization. Using LiMTFSI (lithium 3-[(trifluoromethane)-sulfonamidosulfonyl]propyl methacrylate) as a single-ion source and PEGM and PEGDM as precursors, they systematically varied cross-linking density and EO/Li ratio.[63] Their findings revealed that lower glass transition temperatures and storage moduli correspond to higher ionic conductivity, emphasizing the importance of polymer chain flexibility and weak Li$^+$ coordination. The SPEs achieved conductivity up to 10^{-5} S cm^{-1} and transport numbers approaching unity, with excellent thermal stability and mechanical integrity. This work highlights the delicate balance between mechanical strength and ion mobility in designing high-performance crosslinked PEO-based electrolytes.

Taken together, these studies illustrate the diverse strategies available for crosslinking PEO-based polymer electrolytes, each contributing to improved ionic conductivity, mechanical resilience, and thermal stability. Whether through UV-induced curing, ROMP, thiol–ene photopolymerization, electrospinning, or radical copolymerization, crosslinked architectures consistently suppress crystallinity and enhance segmental mobility—key factors for efficient ion transport. The integration of ionic liquids, dual-salt systems, and functional nanofillers further expands the design space, enabling tailored performance across a range of operating conditions. These insights pave the way for composite and hybrid polymer systems, where interfacial engineering and multifunctional components can synergistically elevate solid-state electrolyte performance.

4. Comparative perspective on polymer architectures

Block, graft, and crosslinked polymers represent three distinct polymerization strategies for tailoring the performance of PEO-based solid polymer electrolytes, each influencing ionic transport, mechanical robustness, and thermal stability in unique ways. Block copolymers exploit microphase separation to generate ordered domains, where soft PEO-rich regions facilitate ion conduction while rigid blocks provide mechanical reinforcement. This architecture partially suppresses PEO crystallinity, though residual crystalline domains can persist depending on block composition and purity, which may limit conductivity at lower temperatures. Graft copolymers, by contrast, introduce flexible side chains onto a rigid backbone, disrupting chain packing more effectively and thereby reducing crystallinity to enhance segmental mobility. Their synthetic versatility allows fine-tuning of graft density and backbone rigidity, enabling a balance between conductivity and mechanical strength, though excessive grafting can compromise modulus. Crosslinked polymers form three-dimensional covalent networks that strongly suppress crystallinity, yielding fully amorphous systems with excellent dimensional and thermal stability. While the restricted chain dynamics in such networks often reduce ionic conductivity compared to block or graft systems, their superior mechanical integrity and resistance to thermal deformation make them particularly attractive for safety-critical applications such as high-voltage or

Table 2 Influence of different polymerization techniques on the property of the PEO-based SPEs

Properties	Block copolymers	Graft copolymers	Crosslinked polymers
Morphology	Microphase separation into ordered domains (*e.g.*, lamellae, cylinders)	Grafted side chains on a backbone; morphology often less ordered but tunable	3D network structure with covalent crosslinks; amorphous but mechanically robust
Ionic conductivity	Enhanced *via* soft PEO-rich domains; depends on block ratio and domain size	Improved segmental mobility; tunable *via* graft density and backbone rigidity	Often lower due to restricted chain mobility; stable under high voltage and temperature
Mechanical strength	Moderate; depends on hard block fraction (*e.g.*, PS or PMMA)	Backbone provides strength; excessive grafting may reduce modulus	High; crosslinking suppresses crystallinity and enhances dimensional stability
Thermal stability	Improved relative to neat PEO; hard blocks resist flow at elevated temperatures	Backbone chemistry dictates stability; grafting can improve T_g and suppress crystallization	Excellent; crosslinked networks resist thermal deformation and maintain integrity
Crystallinity	Partial suppression; PEO blocks may retain crystallinity depending on domain purity	Reduced crystallinity due to disrupted chain packing from grafted side chains	Strongly suppressed; crosslinking disrupts PEO chain ordering, yielding fully amorphous systems
Applications	High-performance electrolytes with balanced conductivity and mechanical strength	Flexible design for optimizing ion transport and mechanical balance	Safety-critical applications needing dimensional stability and flame retardancy

flame-retardant battery designs. Collectively, these architectures underscore the trade-offs between conductivity, crystallinity suppression, and mechanical resilience, highlighting the need for rational hybrid or multi-architecture approaches that integrate structural control with electrochemical performance. To clearly illustrate these distinctions, Table 2 summarizes the comparative properties of block, graft, and crosslinked polymers in terms of morphology, ionic conductivity, mechanical strength, thermal stability, crystallinity, and potential applications.

5. Composite polymers

Composite polymer electrolytes represent one of the most versatile and widely explored strategies for enhancing the performance of poly(ethylene oxide) (PEO)-based solid polymer electrolytes. By incorporating functional fillers into the polymer matrix, researchers have been able to simultaneously improve ionic conductivity, mechanical stability, and interfacial compatibility with electrodes. The choice of filler—whether organic, inorganic, or ionic liquid—plays a decisive role in tailoring the microstructure and transport properties of the composite. Organic fillers often provide flexibility and improved segmental dynamics, inorganic fillers contribute to mechanical reinforcement and ion transport pathways, and ionic liquid additives introduce unique physicochemical environments that facilitate ion dissociation and mobility. Together, these approaches highlight the adaptability of composite design and underscore its importance in advancing PEO-based electrolytes toward practical solid-state battery applications.

5.1. Composite with organic fillers

Organic fillers have emerged as versatile additives for PEO-based solid polymer electrolytes, offering pathways to simultaneously enhance ionic conductivity, mechanical strength, and safety. Their effectiveness stems from disrupting polymer crystallinity, promoting amorphous regions, and introducing functional sites that facilitate ion transport and interfacial stability. Wang *et al.* demonstrated this principle using hydrolyzed polymaleic anhydride (HPMA), where strong Lewis acid–base interactions between carboxyl groups and PEO ether oxygens suppressed crystallinity and boosted conductivity to 1.13×10^{-4} S cm^{-1} at 35 °C.[64] The resulting cells cycled stably for over 1250 cycles, underscoring HPMA's multifunctionality in flexible and safe battery designs. Building on this concept of dual functionality, Zeng *et al.* introduced zinc bis(2-ethylhexanoate) [Zn(BEH)$_2$], which not only disrupted PEO crystallinity but also formed an *in situ* LiZn alloy interphase.[65] This interfacial engineering suppressed dendrites and enabled symmetric Li/Li cells to cycle for 500 hours, highlighting how organic fillers can simultaneously address bulk and interfacial limitations. The resulting PEO-Zn(BEH)$_2$ composite achieved a conductivity of 2.7×10^{-4} S cm^{-1} at 60 °C and a tLi$^+$ of 0.5, demonstrating the synergistic benefits of interfacial engineering and polymer matrix modification.

Expanding beyond small-molecule additives, Sun *et al.* employed HKUST-1 metal–organic frameworks (MOF) as multifunctional fillers (HKUST-1 is composed of Cu^{2+} ions and bezene-1,3,5-tricarboxylate linkers).[66] Their open metal sites captured TFSI$^-$ anions, increasing lithium-ion transference numbers while reducing crystallinity. The resulting composites achieved conductivities up to 2.4 x10^{-3} S cm^{-1} at 80 °C and improved fire safety, demonstrating how MOFs can integrate electrochemical and thermal benefits. Similarly, Ahn *et al.* explored adenine-based bio-MOFs, which provided both Lewis acidic and basic sites.[67] At 3 wt% loading, the composite achieves high conductivity (5.7×10^{-4} S cm^{-1} at 60 °C) and a wide electrochemical window (4.57 V). The fillers reduce PEO crystallinity and improve chain mobility. The transference number increases from 0.47 to 0.63 (Fig. 5A). Full-cell tests with $LiFePO_4$ show high capacity and stable cycling. Overall, bio-MOFs are promising for high-performance solid-state lithium batteries.

Sustainability was further emphasized by Aziam *et al.*, who incorporated phosphorylated cellulose nanofibers (CNF-P).[68]

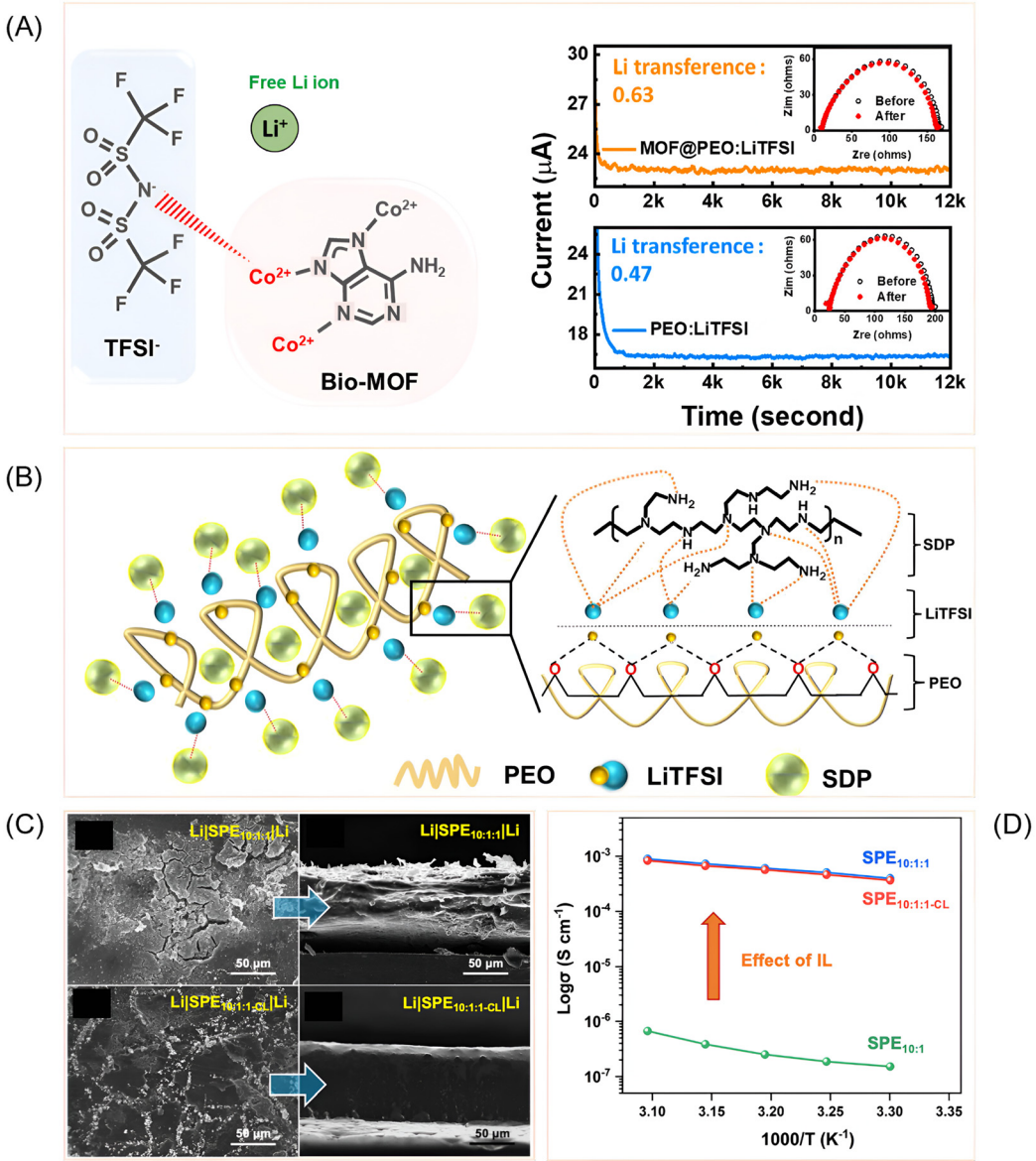

Fig. 5 (A) Interaction between the LiTFSI and Bio-MOF (left) and the enhancement of the lithium transference number with the MOF incorporation to the polymer matrix (right). Reprinted with permission from ref. 67. Copyright (2023) Elsevier. (B) Schematic illustration of Li^+ ion migration pathway in PEO-LiTFSI-SDP solid electrolyte. Reprinted with permission from ref. 76. Copyright (2023) Elsevier. (C) SEM images of Li metal with linear (top) and crosslinked (bottom) SPE with ionic liquid. Reprinted with permission from ref. 85 under a Creative Commons Attribution (CC-BY-NC-ND) License 4.0. (D) Effect of ionic liquid in enhancing the ionic conductivity of SPE. Reprinted with permission from ref. 85 under a Creative Commons Attribution (CC-BY-NC-ND) License 4.0.

Beyond reinforcing mechanical strength (tensile strengths up to 45 MPa), CNF-P imparted flame-retardant properties and broadened electrochemical stability windows above 5 V, illustrating the dual role of bio-based fillers in safety and performance. The composite electrolytes exhibited ionic conductivities exceeding 10^{-4} S cm^{-1} at 70 °C. These features enabled stable cycling in $Li/LiFePO_4$ cells, demonstrating the dual role of CNF-P in enhancing both safety and performance. Complementing these approaches, Chen and Han *et al.* integrated a cationic covalent organic framework (EB-COF-TFSI; EB: ethidium bromide) into PEO matrices.[69] The cationic framework facilitated Li^+ transport by immobilizing $TFSI^-$ anions and promoting salt dissociation, leading to a high lithium-ion transference number (tLi^+ = 0.316) and ionic conductivity of 2.19×10^{-4} S cm^{-1} at 50 °C. Notably, the optimized 1 wt% EB-COF-TFSI loading yielded the best performance, while higher loadings led to increased interfacial resistance and reduced conductivity. The composite electrolyte supported both Li metal and graphite anodes, with graphite-based cells outperforming their Li counterparts in rate capability and cycling stability, offering a practical pathway toward commercial all-solid-state batteries.

5.2. Composite with inorganic fillers

Inorganic fillers have been widely employed to address the intrinsic limitations of PEO-based solid polymer electrolytes, particularly their high crystallinity and low room-temperature conductivity. By introducing ceramic oxides, garnet-type electrolytes, sulfides, and nanostructured materials into the polymer matrix, researchers have demonstrated significant improvements in ionic transport, mechanical strength, and interfacial stability. Chen *et al.* explored garnet-type LLZTO ($Li_{6.4}La_3Zr_{1.4}Ta_{0.6}O_{12}$) fillers in both "ceramic-in-polymer" and "polymer-in-ceramic" configurations.[70] The optimal 10 wt% LLZTO loading in PEO yielded the highest ionic conductivity (1.58×10^{-3} S cm^{-1} at 80 °C) and stable cycling in $LiFePO_4$‖Li cells. The addition of PEG (polyethylene glycol) improved flexibility and thermal stability, enabling robust membranes suitable for high-voltage applications. Adding a sustainable perspective, Xu *et al.* introduced a novel filler derived from waste eggshells (FDE), primarily composed of CaO.[71] The submicron FDE particles reduced PEO crystallinity and enhanced ionic conductivity (6.39×10^{-5} S cm^{-1} for Li^+ and 4.9×10^{-5} S cm^{-1} for Na^+ at RT). The composite electrolytes also exhibited improved mechanical strength and electrochemical stability (up to 5 V), supporting long-term cycling in both $LiFePO_4$ and $Na_3V_2(PO_4)_3$ cells.

Filler particle size effects were further clarified by Song *et al.*, who examined LLZTO using ^{7}Li NMR.[72] Ball-milled LLZTO (BM-LLZTO) with smaller particle size and higher surface area facilitated faster interfacial Li^+ migration, yielding a higher transference number (0.272 *vs.* 0.144) and ionic conductivity (6.0×10^{-5} S cm^{-1} *vs.* 4.6×10^{-5} S cm^{-1}). The BM-LLZTO CSEs also exhibited lower overvoltage and better rate performance in $LiFePO_4$‖Li cells. Reinforcing the importance of morphology, Ramkumar *et al.* investigated ternary oxide $Li_2O{\cdot}SiO_2{\cdot}TiO_2{\cdot}P_2O_5$ (LSTP).[73] Nanoparticles (~300 nm) outperformed micron-sized fillers in reducing PEO crystallinity and enhancing ionic conductivity (1.09×10^{-3} S cm^{-1} at 80 °C). $LiFePO_4$‖Li cells with nano-LSTP CPEs delivered 110 mA h g^{-1} after 100 cycles at 1C and 60 °C, demonstrating the critical role of nanoscale engineering.

Moving beyond oxides, Chen *et al.* explored porous sulfide fillers, specifically $Li_{4.7}Ag_{1.63}GeS_{4.8}$ (LAGS).[74] The unique porous structure of LAGS provided channels that redirected lithium dendrite growth, effectively mitigating short-circuit risks. The composite electrolyte achieved an ionic conductivity of 1.36×10^{-4} S cm^{-1} at 40 °C and supported stable cycling over 555 hours in symmetric Li cells. $LiFePO_4$‖Li cells retained 160.65 mA h g^{-1} after 200 cycles with 99.93% coulombic efficiency. Exploring dual-filler strategies, Lv *et al.* combined nanostructured $LiAlO_2$ (LAO) and polyacrylonitrile (PAN) in a PEO matrix to form a composite electrolyte.[75] LAO reduced crystallinity and enhanced ionic conductivity (3.60×10^{-4} S cm^{-1} at 60 °C), while PAN formed a Li_3N-rich interphase with lithium metal, reducing interfacial impedance. Symmetric Li cells cycled stably for 1000 hours, and $LiFePO_4$‖Li cells retained 92% capacity after 200 cycles.

Surface modification has also proven effective. Wang *et al.* developed a surface-modified SiO_2 filler coated with dopamine and branched polyethyleneimine (SDP: abbreviation for the filler), which introduced a positively charged interface that enhanced lithium salt dissociation and reduced PEO crystallinity (Fig. 5B).[76] The resulting PEO-LiTFSI-SDP composite achieved an ionic conductivity of 6.12×10^{-5} S cm^{-1} at 30 °C and a lithium transference number of 0.46. The modified filler also facilitated the formation of a LiF-rich interphase, enabling stable cycling over 3960 hours in symmetric Li cells and 260 cycles in $LiFePO_4$ cells with 92.8% capacity retention. To complement these approaches, Yin *et al.* introduced an *in situ* synthesized SiO_2 filler within a PEO matrix (I-PEO-SiO_2), forming strong chemical bonds between filler and polymer.[77] This method resolved interfacial compatibility issues and suppressed sodium dendrite formation. The I-PEO-SiO_2 electrolyte exhibited a high Na^+ conductivity of 2.3×10^{-4} S cm^{-1} at 60 °C and a transference number of 0.46. $Na_3V_2(PO_4)_3$‖Na cells demonstrated ultra-long cycling stability over 4000 cycles and high-rate capability, outperforming *ex situ* mixed systems.

5.3. Composite polymer with ionic liquids (ILs)

ILs have emerged as powerful additives in composite polymer electrolytes, offering unique advantages such as high ionic conductivity, wide electrochemical stability windows, and intrinsic safety features. Their incorporation into PEO-based systems disrupts crystallinity, enhances lithium salt dissociation, and improves mechanical and thermal stability, making them versatile tools for advancing solid-state battery performance. One promising approach involved the incorporation of imidazolium-based polyhedral oligomeric silsesquioxane ionic liquids (POSS-ILs), as demonstrated by Shang *et al.*[78] The POSS-ILs uniformly dispersed in the polymer matrix, significantly suppressing crystallinity. Among the variants, POSS-PrMIM (PrMIM: propyl-substitute methyl imidazolium) SPE exhibited the highest ionic conductivity (3.9×10^{-4} S cm^{-1} at 22 °C and 1.5×10^{-3} S cm^{-1} at 62 °C), with enhanced amorphous character and ion mobility. The electrochemical stability window extended up to 5.0 V, and the SPEs demonstrated excellent dimensional and thermal stability under elevated temperatures. Building on this concept of embedding ionic liquids directly into polymer frameworks, Li *et al.* prepared a semi-interpenetrating polymer network (semi-IPN) electrolyte.[79] The ionic liquid monomer 1-vinyl-3-methylimidazolium bis(trifluoromethylsulfonyl)imide ([VMIM]TFSI) was polymerized with poly(ethylene glycol) diacrylate (PEGDA) in the presence of PEO and LiTFSI, forming a flexible membrane with reduced crystallinity (15.5%) and improved ionic conductivity (6.12×10^{-4} S cm^{-1} at 55 °C). The PIL (polymeric ionic liquid) network promoted lithium salt dissociation while maintaining mechanical integrity and thermal stability up to 280 °C. The electrolyte exhibited a wide voltage stability window (5.44 V) and delivered high reversible capacity (147 mA h g^{-1} at 0.2 C) with stable cycling in $LiFePO_4$‖Li cells.

Extending the scope to bio-derived ionic liquids, Tan *et al.* incorporated a biomass-based poly(ionic liquid) hydroxypropyl

trimethylammonium bis(trifluoromethane) sulfonimide chitosan salt (HACC-TFSI).[80] This polycationic additive reduced crystallinity, enhanced salt dissociation, and improved conductivity and thermal stability. The optimized system achieved ionic conductivities of 1.77×10^{-5} S cm^{-1} at 30 °C and 5.01×10^{-4} S cm^{-1} at 60 °C, with a transference number of 0.34. It also demonstrated superior mechanical strength and dimensional stability, retaining 97% capacity after 100 cycles at 60 °C and maintaining 73% capacity at 150 °C, where blank SPEs failed. Taking a hybrid approach, Hu *et al.* combined graphene oxide (GO) with an ionic liquid (IL) 1-butyl-3-methylimidazolium dicyanamide ([BMIM][DCA]) to form a co-doped system (PGI: PEO, GO, IL).[81] GO and IL synergistically reduced crystallinity and formed a 3D cross-linked network that immobilized anions, increasing lithium-ion transference (0.52) and suppressing dendrites. PGI achieved ionic conductivity of 10^{-4} S cm^{-1} at 30 °C, excellent thermal stability up to 350 °C, and a wide stability window of 4.8 V. Symmetric Li||Li cells cycled stably for over 1800 hours, while $LiFePO_4$||Li cells retained 98.6% capacity after 100 cycles.

Advancing this idea of layered architecture, Cai *et al.* developed a multilayered composite electrolyte.[82] The multilayered structure consisted of a central PEO–LLZTO layer sandwiched between ionic-liquid-containing polymer interlayers (PVDF-HFP, LiTFSI, PYR13TFSI). This design enhanced interfacial stability with both high-voltage cathodes and lithium metal anodes. The IL-containing interlayers exhibited high conductivity (3.91×10^{-4} S cm^{-1}), low activation energy (0.23 eV), and stability up to 4.5 V. Symmetric Li/Li cells cycled stably for over 1000 hours, while full cells delivered high capacities with >82% retention after 100 cycles. In parallel, Lei *et al.* explored ionic liquid-grafted ZIF-90 nanofillers (ZIF-90-*g*-IL) dispersed into a PEO matrix (ZIF: zeolitic imidazolate framework-90).[83] The composite achieved high conductivity (1.17×10^{-4} S cm^{-1} at 30 °C), a wide stability window (4.8 V), and a transference number of 0.44. Symmetric Li/Li cells cycled stably for over 700 hours, while $LiFePO_4$/Li and NCM811/Li cells demonstrated excellent cycling stability and capacity retention.

Complementing these experimental advances, Arya and Gupta provided theoretical insights using DFT to study nitrogen-rich ionic liquid [EMIMDCA] (EMIMDCA: 1-ethyl-3-methylimidzolium dicyanamide) in PEO-LiTFSI matrices.[87] Incorporation of [EMIMDCA] reduced the HOMO–LUMO gap (3.25 → 2.80 eV), enhanced ion mobility, and improved electrochemical reactivity. Strong interactions between PEO oxygen atoms, Li^+ cations, and DCA^- anions facilitated smoother ion migration, highlighting the mechanistic role of ILs in transport.

Further expanding multifunctionality, Zhu *et al.* developed a flexible, flame-retardant, and self-healing SPE by integrating imidazolium-based polymer ionic liquid@PEGMA block polymerized with PEO.[86] The microphase-separated architecture reduced crystallinity and facilitated transport, achieving conductivity of 2.2×10^{-4} S cm^{-1} and a transference number of 0.63. The BPIL (block polymerized ionic liquid) framework enabled intrinsic self-healing within 30 minutes at 60 °C and strong adhesion to lithium metal. $LiFePO_4$/Li cells delivered 163 mA h g^{-1} and retained 81% capacity after 50 cycles. Reinforcing the role of ILs in conductivity enhancement, Polu *et al.* doped PEO with LiTDI (lithium 4,5-dicyano-2-(trifluoromethyl)imidazole) and EMImTFSI (1-ethyl-3-methylimidazolium bis(trifluoromethylsulfonyl)-imide).[84] The optimized composition achieved conductivity of $\sim 1.78 \times 10^{-4}$ S cm^{-1} at 60 °C, thermal stability up to 300 °C, and a stability window of ~4.2 V. Strong interactions among PEO, LiTDI, and EMImTFSI reduced crystallinity and increased amorphous content. $LiFePO_4$/Li cells delivered 161 mA h g^{-1} initially and retained 145.5 mA h g^{-1} after 50 cycles. To complement these approaches, Zhang *et al.* introduced a UV-crosslinked polymer electrolyte with concentrated IL (CIL).[85] The SPE consists of PEO, *N*-propyl-*N*-methylpyrrolidinium bis(fluorosulfonyl)imide (C_3mpyrFSI) and LiFSI salt. The CIL incorporated SPE not only protects the Li surface, also greatly enhances the ionic conductivity (Fig. 5C and D). Crosslinking reduced crystallinity and enhanced IL uptake, yielding conductivity of $\sim 4 \times 10^{-4}$ S cm^{-1} at 30 °C and stability up to 4.9 V. Cycling tests showed suppressed dendrites and >90% capacity retention in Li||LFP and Li||LMO cells.

In summary, composite polymer electrolytes that combine organic matrices, inorganic fillers and ionic liquids demonstrate complementary advantages for PEO-based systems. Table 3 compares the ionic conductivity of each polymer with variation in the filler materials. The organic phase ensures flexibility and ease of processing, inorganic components reduce crystallinity and strengthen mechanical integrity, and ionic liquids enhance ionic conductivity while improving interfacial stability. Together, these elements create hybrid structures that achieve a balance between mechanical robustness and electrochemical performance, underscoring their potential as practical solid-state electrolyte designs.

6. Salt design strategies

The design of lithium salts plays a central role in tailoring the performance of PEO-based solid polymer electrolytes. Beyond serving as simple ion sources, engineered salts can disrupt polymer crystallinity, enhance lithium-ion dissociation, and stabilize electrode interfaces. Recent advances highlight strategies ranging from polyanion frameworks to dual-salt systems and polymer-in-salt architectures, each contributing unique benefits to conductivity, stability, and cycling performance. Single-ion conducting SPEs are being focused due to their resistance toward concentration polarization and higher Li^+ transference number compared to the ual-ion conducting electrolytes (Fig. 6B). The introduction of lithium poly[(cyano)(4-styrenesulfonyl)imide] (LiPCSI) was reported by Yuan *et al.*,[88] a polyanion featuring a sulfonylimide core and a cyano group tethered to a polystyrene backbone. The cyano group enhanced oxidation resistance (up to 5.53 V *vs.* Li^+/Li), while the polystyrene backbone dispersed negative charge and reduced crys-

Table 3 PEO-based SPEs with different filler materials and their ionic conductivities

Filler type	Composition	Filler	Ionic conductivity (S cm^{-1})	Work
Organic	PEO-HPMA	HPMA (hydrolyzed polymaleic anhydride)	1.13×10^{-4} (35 °C)	Wang *et al.*[64]
	PEO-(bio-MOF)	Adenine-Co(II) bio-MOF	5.7×10^{-4} (60 °C)	Ahn *et al.*[67]
	PEO-(CNF-P)	CNF-P (phosphorylated cellulose nanofibers)	$\sim 10^{-4}$ (70 °C)	Aziam *et al.*[68]
	PEO-(EB-COF-TFSI)	EB (ethidium bromide), COF (covalent organic framework), TFSI (bis(trifluoromethanesulfonyl)imide)	2.19×10^{-4} (50 °C)	Chen & Han *et al.*[69]
	PEO-$Zn(BEH)_2$	$Zn(BEH)_2$ (zinc bis(2-ethylhexanoate))	2.7×10^{-4} (60 °C)	Zeng *et al.*[65]
	PEO-(HKUST-1)	HKUST-1 ($[Cu_3(BTC)_2(H_2O)_3]$, BTC: 1,3,5-benzenetricaboxylate)	2.4×10^{-4} (80 °C)	Sun *et al.*[66]
Inorganic	PEO-SDP	SDP (SiO_2 coated with polydopamine and branched polyethyleneimine)	6.12×10^{-5} (30 °C)	Wang *et al.*[76]
	PEO-SiO_2	*In situ* synthesized SiO_2	2.3×10^{-4} (60 °C)	Yin *et al.*[77]
	PEO-LAGS	LAGS ($Li_{4.7}Ag_{1.63}GeS_{4.8}$)	1.36×10^{-4} (40 °C)	Chen *et al.*[74]
	PEO-LAO-PAN	LAO ($LiAlO_2$), PAN (polyacrylonitrile)	3.6×10^{-4} (60 °C)	Lv *et al.*[75]
	PEO-LSTP	LSTP (Li_2O, SiO_2, TiO_2, P_2O_5)	1.09×10^{-3} (80 °C)	Ramkumar *et al.*[73]
	PEO-LLZTO	LLZTO (tantalum-doped lithium lanthanum zirconium oxide)	1.58×10^{-3} (80 °C)	Chen *et al.*[70]
	PEO-CaO	CaO from eggshell	6.39×10^{-5} (RT)	Xu *et al.*[71]
Ionic liquid (IL)	IPL-PLL-IPL	PYR_{13}TFSI (*N*-methyl-*N*-propylpyrrolidinium bis(trifluoro-methanesulfonyl)imide)	1.75×10^{-4} (RT)	Cai *et al.*[82]
	PEO-GO-IL	[BMIM][DCA] (1-butyl-3-methylimidazolium dicyanamide)	$\sim 10^{-4}$ (30 °C)	Hu et. al.[81]
	PEO-(ZIF-90-*g*-IL)	ZIF-90-*g*-IL (zeolitic imidazolate framework-90 nanofiller grafted with imidazole IL containing siloxane groups	1.17×10^{-4} (30 °C)	Lei *et al.*[83]
	PEO-PIL	[VMIM]TFSI (1-vinyl-3-methyl-imidazolium bis(trifluoromethyl-sulfonyl)imide)	6.12×10^{-4} (55 °C)	Li *et al.*[79]
	PEO-EMImTFSI	EMImTFSI (1-ethyl-3-methyl-imidazolium bis(trifluoro-methylsulfonyl)imide	1.78×10^{-4} (60 °C)	Polu *et al.*[84]
	PEO-P(VDF-HFP)-PC-(POSS-IL)	POSS-IL (polyhedral oligomeric silsesquioxane ionic liquid)	1.5×10^{-3} (62 °C)	Shang *et al.*[78]
	PEO-(HAAC-TFSI)	HAAC-TFSI (hydroxypropyl trimethylammonium bis (trifluoromethane)sulfonimide chitosan salt)	5.01×10^{-4} (60 °C)	Tan *et al.*[80]
	PEO-(C_3mpyrFSI)	C_3mpyrFSI (*N*-propyl-*N*-methyl-pyrrolidinium bis(fluoro-sulfonyl) imide	4×10^{-4} (RT)	Zhang *et al.*[85]
	PEO-BPIL	BPIL (imidazolium-based polymerized IL@PEGMA block polymer)	2.2×10^{-4} (60 °C)	Zhu *et al.*[86]

tallinity. The resulting PEO-*g*-LiPCSI SPE achieved a high $t\mathrm{Li}^+$ of 0.84 and demonstrated stable cycling over 1000 hours in symmetric Li cells.

Building on the concept of single-ion conductors, Martinez-Ibañez *et al.* showed that adding just 2 wt% of LiFSI to a LiPSTFSI/PEO (LiPSTFSI: lithium poly[(4-styrenesulfonyl) (trifluoromethane–sulfonyl)imide]) matrix significantly improved ionic conductivity (Fig. 6C and D) and interfacial stability.[89] This additive-containing single lithium-ion conductor (ACSLIC) maintained high $t\mathrm{Li}^+$ and formed a LiF-rich SEI, enhancing compatibility with lithium metal and enabling stable cycling in $LiFePO_4$ cells. Further advancing single-ion systems, Li *et al.* developed a crosslinked borate-based network (PTF-4EO) by reacting LiCTFPB (lithium tetrakis(4-(chloromethyl)-2,3,5,6-tetrafluorophenyl)borate) salt with tetraethylene glycol.[90] The weak anion–Li^+ interactions and ether oxygen coordination delivered high conductivity (3.53×10^{-4} S cm^{-1}), $t\mathrm{Li}^+ = 0.92$, and a wide electrochemical window (>4.8 V). The electrolyte also enabled stable cycling in LFP and NMC pouch cells under harsh conditions. Complementing these approaches, Lu *et al.* proposed incorporating zwitterions as synergistic ion dissociators and phase plasticizers to enhance single lithium-ion conducting SPEs (SLICSPEs).[91] Using monomeric MIPS (3-(1-methyl-3-imidazolio)propanesulfonate) and polymeric VIPS (3-(1-vinyl-3-imidazolio)propanesulfonate) in PEO matrices containing polyanionic salts (PLSS and LiPSTFSI), they facilitated Li^+ dissociation and reduced crystallinity (PLSS: poly(lithium 4-styrenesulfonate)) (Fig. 6A). Spectroscopic analyses confirmed strong zwitterion–polyanion interactions, while DSC and XRD showed that VIPS lowered crystallinity more effectively than MIPS. The optimized LiPSTFSI + VIPS/PEO system achieved conductivity of 8.39×10^{-5} S cm^{-1} at 90 °C and a transference number close to unity, with stable cycling in $LiFePO_4$/SLICSPE/Li cells.

Exploring alternative architectures, Zhao *et al.* investigated a biphasic SPE composed of poly(ethylene carbonate) and PVDF-HFP (poly(vinylidene fluoride-*co*-hexafluoropropane)), forming a "polymer-in-salt" structure with dual Li^+ transport pathways.[92] Although based on a single salt (LiTFSI), the design mimicked dual-ion behavior and achieved conductivity of 1.08×10^{-4} S cm^{-1} at 30 °C, with stable cycling with $LiFePO_4$ cathode. Expanding this polymer-in-salt concept, Zhang *et al.* incorporated LiFSI into a PVDF-HFP matrix with LLZTO filler,[93] achieving ultrahigh conductivity (1.67×10^{-3} S cm^{-1}), a critical current density of 3.2 mA cm^{-2}, and excellent interfacial stability with lithium metal. This demonstrated the potential of high-salt-content dual-ion systems. Taking a rational design approach, Li *et al.* applied a phase diagram-guided strategy to develop a dual-salt SPE combining LiTFSI and LiBOB (lithium bis(oxalate)borate) with glutaronitrile

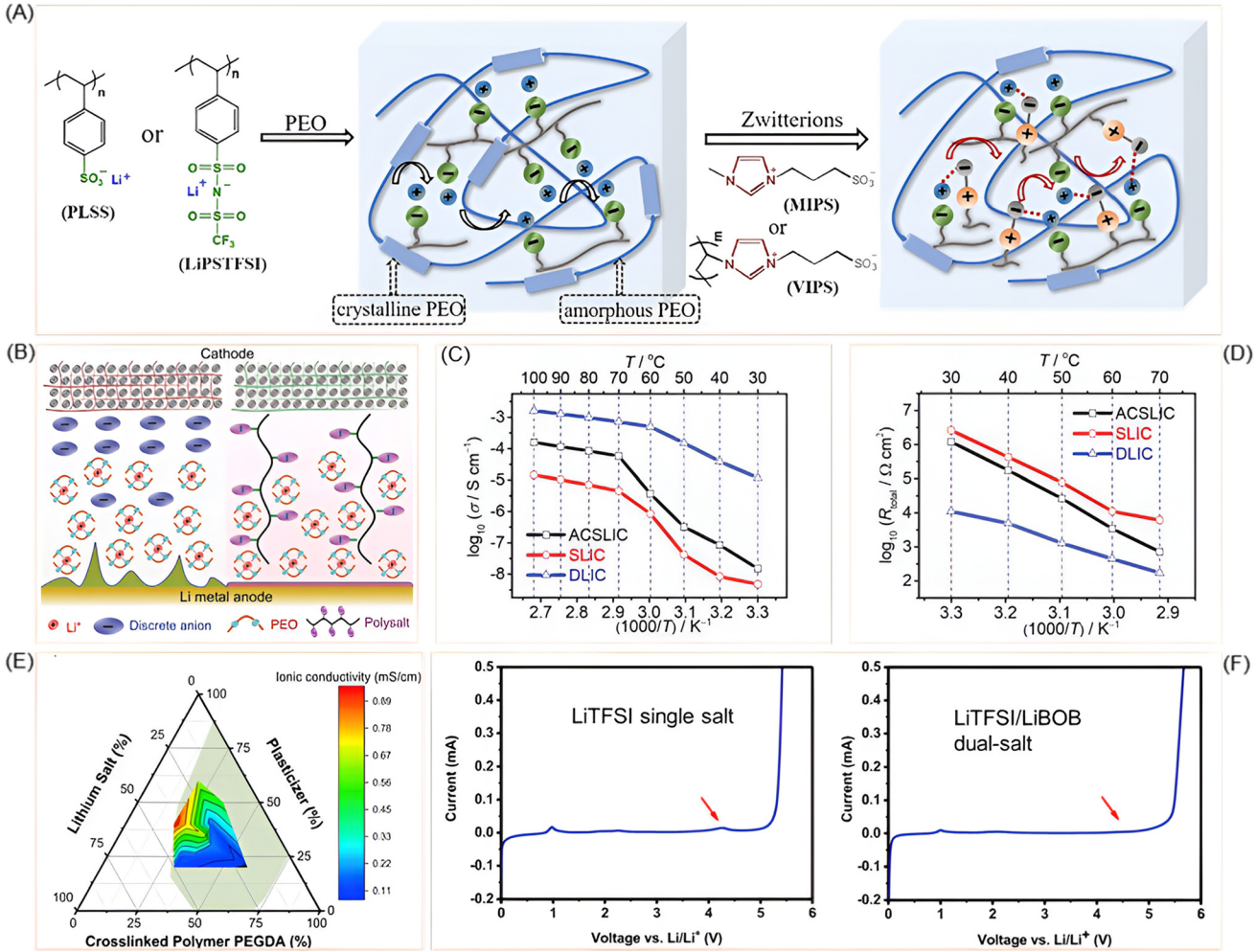

Fig. 6 (A) Schematic representation of Li^+ ion dissociation in SLIC and PEO/Zwitterion blended polymer. Reprinted with permission from ref. 91. Copyright (2020) Elsevier. (B) An illustration to differentiate between single and dual-ion conducting polymer electrolytes. Reprinted with permission from ref. 89. Copyright (2020) John Wiley & Sons. (C) Ionic conductivity and (D) resistance comparison between single lithium-ion conducting SPE with (ACSLIC) and without (SLIC) additive LiFSI. Reprinted with permission from ref. 89. Copyright (2020) John Wiley & Sons. (E) Ternary phase diagram of SPE with the ionic conductivity. Reprinted with permission from ref. 94. Copyright (2018) Elsevier. (F) Stability comparison between SPE with single and dual salt formulation, where dual salt containing SPE shows better stability at higher voltage. Reprinted with permission from ref. 94. Copyright (2018) Elsevier.

plastic crystal and PEGDA host (Fig. 6E).[94] The optimized composition achieved conductivity up to 1.0 mS cm^{-1} at 30 °C, a transference number of ~0.75, and stability up to 4.5 V *vs.* Li^+/Li. From the LSV (Fig. 6F), it is discernible that the LiTFSI/LiBOB dual-salt formulation is more stable at higher voltage compared to LiTFSI single salt. Lithium stripping/plating tests showed over 1300 hours of stable cycling, while $LiFePO_4$ cells retained 86% capacity after 370 cycles. Thermal analysis confirmed stability up to 100 °C, making it suitable for elevated-temperature applications. In a related effort, Yu *et al.* developed a solid-like dual-salt polymer electrolyte (DSPE) using LiTFSI and LiBOB in a PVDF matrix, achieving conductivity of 0.73 mS cm^{-1} at room temperature and 1.93 mS cm^{-1} at 100 °C.[95] The dual-salt formulation stabilized the Al current collector and formed a robust LiF-rich SEI, enabling stable cycling across a wide temperature range (−10 °C to 80 °C). Pushing the boundaries of dual-salt systems, Lee *et al.* introduced a dual-salt/dual-supporter strategy by combining [EMIM][TFSI] and LiTFSI within a PEGDA matrix.[96] This minimized ion-pair formation and achieved conductivity of ~2.4 × 10^{-2} S cm^{-1} at room temperature. The addition of glass fiber mesh and LLTO particles enhanced mechanical strength and ion transport, yielding an elastic toughness of ~170.3 kJ m^{-2}. The SPE demonstrated excellent thermal stability (onset ~300 °C) and low crystallinity, supporting robust performance under mechanical stress.

Together, these studies highlight the evolution of salt design strategies—from polyanion frameworks and zwitterion-assisted single-ion conductors to polymer-in-salt and dual-salt systems. By tailoring anion chemistry, concentration, and synergistic combinations, researchers have achieved remarkable gains in conductivity, transference number, and inter-

facial stability, paving the way for safer and higher-performance solid-state batteries.

7. Flame retardant PEO-based SPEs

Safety is a critical requirement for solid-state batteries, and flame-retardant polymer electrolytes have emerged as an effective strategy to mitigate fire hazards while maintaining electrochemical performance. By integrating flame-retardant additives, structural reinforcements, and novel polymer chemistries into PEO-based matrices, researchers have achieved systems that combine high ionic conductivity with thermal stability and reduced flammability. One innovative approach involved designing a polymer–polymer solid-state electrolyte (SSE), as demonstrated by Cui *et al.* Their system combined a porous polyimide (PI) matrix infused with decabromodiphenyl ethane (DBDPE) as a flame retardant and filled with PEO/

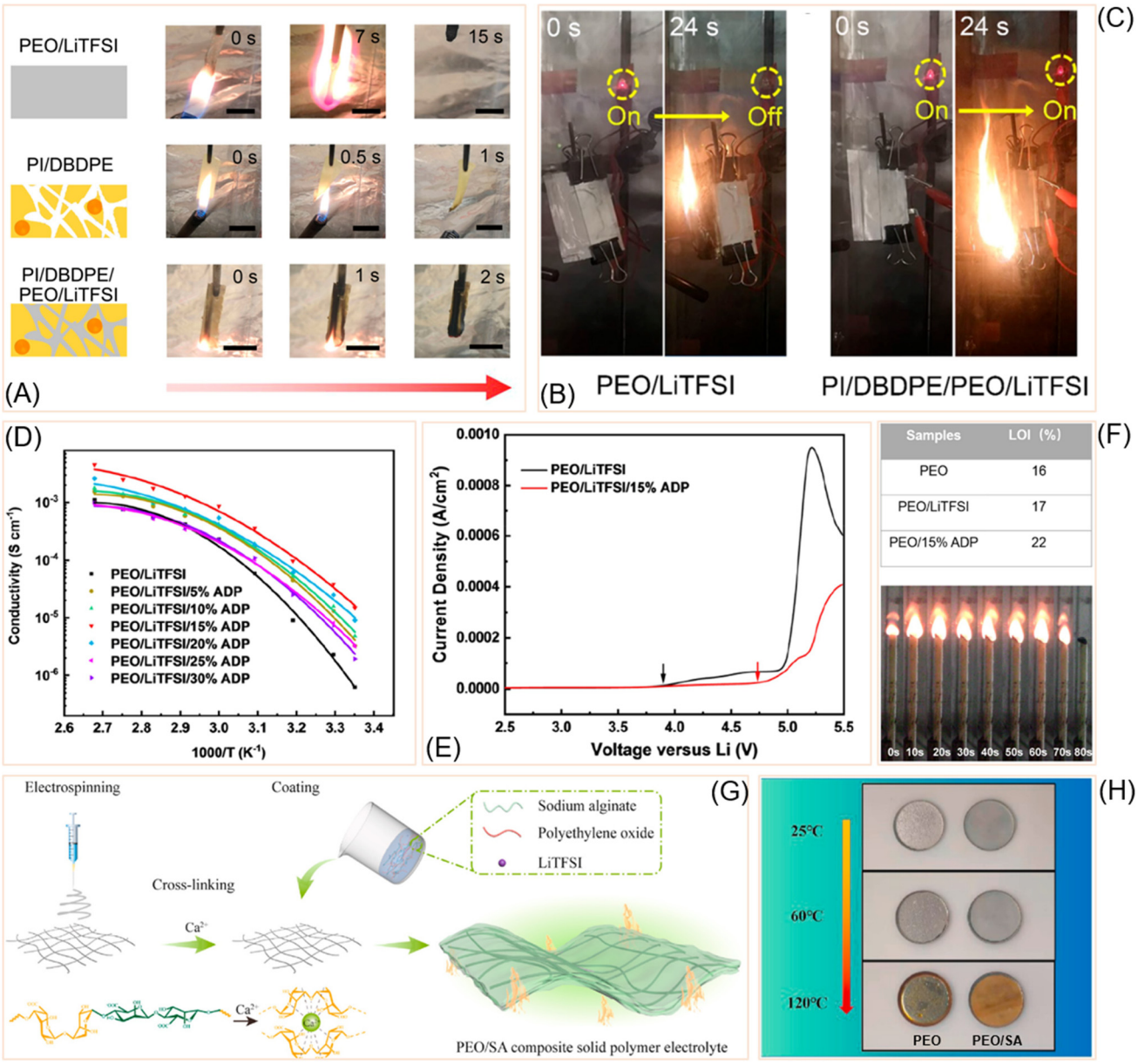

Fig. 7 (A) Flame retardant PI/DBDPE/PEO/LiTFSI solid-polymer electrolyte in flame test. Reprinted with permission from ref. 97. Copyright (2020) American Chemical Society. (B) Thermal abuse test of PEO/LiTFSI and (C) PI/DBDPE/PEO/LiTFSI polymer electrolyte in pouch cell assembly with LFP cathode and LTO anode. Reprinted with permission from ref. 97. Copyright (2020) American Chemical Society. (D) Li^+ ionic conductivity and (E) voltage stability of PEO/LiTFSI solid-polymer electrolyte with ADP additive. Reprinted with permission from ref. 100. Copyright (2021) American Chemical Society. (F) Limiting oxygen index (LOI) and flame test of PEO/ADP solid-polymer electrolyte. Reprinted with permission from ref. 100. Copyright (2021) American Chemical Society. (G) Synthesis scheme of PEO/SA solid electrolyte with (H) high temperature resistivity test. Reprinted with permission from ref. 101. Copyright (2021) Elsevier.

LiTFSI for ionic conductivity.[97] This ultrathin composite exhibited exceptional thermal stability, mechanical strength (~440 MPa), and flame resistance (Fig. 7A), achieving complete self-extinguishment at 15 wt% DBDPE. Electrochemical tests showed superior cycling stability, with pouch cells continuing to function even under flame abuse (Fig. 7B and C). Building on phosphorus-based flame-retardant chemistry, Liu *et al.* developed poly(bis(4-phenoxyl)propane methylphosphonate) (PBMP) as an additive.[98] PBMP raised the limiting oxygen index (LOI) from 15.8% to 25.6% and achieved UL94 V-0 rating at just 3 wt% phosphorus loading. Microcombustion calorimetry revealed reduced heat release, while electrochemical tests showed enhanced conductivity (4.66×10^{-5} S cm^{-1} at 55 °C) and stable cycling in $LiFePO_4$/Li cells. Extending this concept, Olmedo-Martínez *et al.* introduced UV-crosslinked polyphosphoester copolymers that incorporated phosphoester units for fire resistance, PEG segments for salt solvation, and vinyl groups for crosslinking.[99] These copolymers achieved conductivity up to 2×10^{-4} S cm^{-1} at 70 °C, reduced heat release rates, and retained ~80% capacity with >98% coulombic efficiency over 100 cycles.

A halogen-free strategy was pursued by Han *et al.*, who doped PEO/LiTFSI with aluminum diethyl hypophosphite (ADP).[100] At 15 wt% loading, ADP improved conductivity (3.7×10^{-5} S cm^{-1} at 30 °C), widened the stability window (4.7 V), and reduced flammability (LOI from 17% to 22%) (Fig. 7D–F). ADP nanoparticles also formed an Al and P-rich SEI that suppressed dendrite growth, enabling long-term cycling stability. Complementary reinforcement was achieved by Chen *et al.* through electrospun sodium alginate (SA) nanofiber membranes cross-linked with calcium ions (Fig. 7G).[101] The PEO/SA composite SPE exhibited enhanced flame retardancy (LOI = 28.6), thermal stability (>120 °C) (Fig. 7H), and mechanical strength (3.57 MPa). Electrochemical tests showed widened stability windows and 99% capacity retention after 100 cycles. A synergistic design strategy was presented by Zheng *et al.* following the previous works, who integrated a 3D flame-retardant skeleton (3DPA) of PVDF-HFP and ADP with multifunctional Li-ILs@ZIF-8 fillers.[102] The composite achieved high conductivity (2.89×10^{-4} S cm^{-2} at 25 °C), a wide stability window (4.8 V), and excellent dendrite suppression. Cycling tests confirmed >1000 hours of stability in symmetric Li cells and 90% capacity retention after 300 cycles.

Nanostructured flame-retardant additives were explored by Zhao *et al.*, who incorporated black phosphorene (BP) nanosheets as a flame-retardant additive.[103] The authors synthesized BP *via* electrochemical exfoliation and integrated it into a composite electrolyte containing PEO, PVDF, LiTFSI, and nano-Al_2O_3. Remarkably, the optimized formulation with 0.7 wt% BP exhibited significantly improved thermal stability, resisting degradation up to 140 °C, and demonstrated a 62.5% reduction in peak heat release rate compared to pristine PEO-SPE. Electrochemical characterization revealed that BP addition reduced PEO crystallinity, thereby enhancing ionic conductivity to 2.74×10^{-4} S cm^{-1} at 60 °C and extending the electrochemical stability window to 5.9 V. The lithium-ion transference number also increased to 0.53, while electronic conductivity remained low, preserving electrochemical integrity. When applied in all-solid-state lithium-ion batteries (ASSLIBs) with $LiFePO_4$ cathodes, the BP/PEO-SPE membranes delivered superior rate capability, cycling stability, and coulombic efficiency, retaining 92% of capacity after 100 cycles at 0.2 C rate. Ionic liquid integration was combined with polymer reinforcement by Liu *et al.*, who developed an ultra-thin SPE using a polyamide 6 (PA6) electrospun membrane and ionic liquid (HMH: 1-hexyl-3-methylimidazolium hexafluorophosphate).[104] The PA6 membrane reduced crystallinity and improved mechanical strength, while PF_6^- ions provided intrinsic flame-retardant properties ($LiPF_6$ was utilized as the Li^+ source). The optimized composite achieved conductivity of ~10^{-4} S cm^{-1} at 60 °C, a wide voltage stability window (~5.5 V), and excellent cycling stability, retaining 89% capacity after 1800 cycles.

In brief, these studies highlight the diverse and innovative approaches being pursued to engineer flame-retardant SPEs. By integrating functional additives, structural reinforcements, and novel polymer chemistry, researchers have made substantial progress toward safer, high-performance solid-state lithium batteries.

8. Conclusions and future prospect

PEO-based SPEs continue to occupy a central role in the development of next-generation solid-state lithium batteries, owing to their favorable lithium-ion coordination, processability, and cost-effectiveness. Yet, their practical deployment is hindered by several intrinsic limitations, including low ambient-temperature ionic conductivity, narrow electrochemical stability windows, and susceptibility to lithium dendrite formation. This review has systematically examined the diverse strategies employed to overcome these challenges, spanning polymer architecture innovations—such as block copolymers, graft copolymers, crosslinked networks, and composite matrices—as well as functional enhancements through organic and inorganic fillers, ionic liquids, advanced salt chemistries, and flame-retardant motifs. Each design pathway contributes uniquely to improving ion transport, mechanical resilience, interfacial stability, and safety, underscoring the importance of synergistic material engineering.

Among these strategies, the emergence of polymeric ILs, self-healing architectures and flame-retardant functionalities marks a paradigm shift toward multifunctional SPEs that not only perform well electrochemically but also address mechanical and safety concerns. The integration of concentrated ionic liquids and UV-crosslinking, for instance, has demonstrated significant gains in oxidative stability and dendrite suppression, while block copolymer systems offer tunable phase separation and segmental mobility for enhanced conductivity. Furthermore, salt design—particularly single-ion and dual-salt systems—has shown promise in elevating lithium-ion transference numbers and mitigating polarization effects.

Looking forward, the convergence of molecular design with advanced characterization and interfacial engineering presents exciting opportunities. Techniques such as atomic and molecular layer deposition (ALD and MLD),[105,106] synchrotron-based SAXS/WAXS,[107,108] and *in situ* spectroscopic analysis,[109–111] can illuminate nanoscale structure–property relationships and guide rational SPE design. Small-angle and wide-angle X-ray scattering (SAXS and WAXS) provide complementary insights into the multiscale structure of PEO-based solid polymer electrolytes, making them particularly valuable for systems synthesized through diverse polymerization routes. SAXS probes the nanoscale regime, allowing researchers to resolve domain spacing, phase separation, and filler dispersion in block or graft copolymers, thereby clarifying how synthetic strategies influence ion transport pathways. WAXS, on the other hand, captures short-range order and crystallinity, quantifying the balance between amorphous and crystalline fractions that directly govern ionic conductivity. Together, these techniques reveal how polymerization conditions and molecular design alter chain packing, segmental mobility, and salt–polymer interactions. By integrating SAXS and WAXS analyses with synthesis, one can establish predictive correlations between molecular architecture and electrochemical behavior, ensuring that structural engineering translates into functional improvements in solid polymer electrolytes. The development of intrinsically self-healing and flame-retardant SPEs will be critical for flexible, wearable, and high-safety battery platforms. Additionally, machine learning-guided polymer discovery and high-throughput screening may accelerate the identification of optimal PEO-based systems tailored for specific performance metrics. The integration of these approaches with scalable fabrication methods and robust interfacial engineering—especially for lithium metal and high-voltage cathodes—will be pivotal in translating laboratory innovations into commercial solid-state battery technologies.

In summary, the rational design of multifunctional PEO-SPEs—balancing conductivity, stability, mechanical integrity, and safety—will be key to unlocking the full potential of solid-state lithium batteries. Continued interdisciplinary efforts across polymer chemistry, electrochemistry, materials science, and data-driven discovery will shape the future landscape of sustainable and high-performance energy storage.

Author contributions

Taohedul Islam: conceptualization, data curation, formal analysis, investigation, methodology, validation, and writing – original draft; Xiangbo Meng: conceptualization, funding acquisition, project administration, supervision, and writing – review & editing.

Conflicts of interest

The authors declare no competing financial interest.

Data availability

No primary research results, software or code have been included and no new data were generated or analyzed as part of this review.

Acknowledgements

This work was partially supported by U. S. National Science Foundation with the award number of OIA-2429581 and by U. S. Department of Energy, Office of Science, Office of Basic Energy Sciences with the award number of DE-SC0023439. X. M. also appreciates the support of Twenty-First Century Professorship from the University of Arkansas (Fayetteville, Arkansas, USA).

References

1 D. E. Fenton, J. M. Parker and P. V. Wright, Complexes of Alkali Metal Ions with Poly(Ethylene Oxide), *Polymer*, 1973, **14**(11), 589, DOI: 10.1016/0032-3861(73)90146-8.
2 C. Berthier, W. Gorecki, M. Minier, M. B. Armand, J. M. Chabagno and P. Rigaud, Microscopic Investigation of Ionic Conductivity in Alkali Metal Salts-Poly(Ethylene Oxide) Adducts, *Solid State Ion.*, 1983, **11**(1), 91–95, DOI: 10.1016/0167-2738(83)90068-1.
3 M. Li, J. Lu, Z. Chen and K. Amine, 30 Years of Lithium–Ion Batteries, *Adv. Mater.*, 2018, **30**(33), 1800561, DOI: 10.1002/adma.201800561.
4 K. Grandin, *The Nobel Prizes 2019*, World Scientific Publishing Company, 2022.
5 A. K. Stephan, The Age of Li-Ion Batteries, *Joule*, 2019, **3**(11), 2583–2584, DOI: 10.1016/j.joule.2019.11.004.
6 Y. Luo, Z. Rao, X. Yang, C. Wang, X. Sun and X. Li, Safety Concerns in Solid-State Lithium Batteries: From Materials to Devices, *Energy Environ. Sci.*, 2024, **17**(20), 7543–7565, DOI: 10.1039/D4EE02358G.
7 A. C. Luntz, J. Voss and K. Reuter, Interfacial Challenges in Solid-State Li Ion Batteries, *J. Phys. Chem. Lett.*, 2015, **6**(22), 4599–4604, DOI: 10.1021/acs.jpclett.5b02352.
8 Z. Ding, J. Li, J. Li and C. An, Review—Interfaces: Key Issue to Be Solved for All Solid-State Lithium Battery Technologies, *J. Electrochem. Soc.*, 2020, **167**(7), 070541, DOI: 10.1149/1945-7111/ab7f84.
9 S. Kalnaus, N. J. Dudney, A. S. Westover, E. Herbert and S. Hackney, Solid-State Batteries: The Critical Role of Mechanics, *Science*, 2023, **381**(6664), eabg5998, DOI: 10.1126/science.abg5998.
10 Y. Lin, J. Li, K. Liu, Y. Liu, J. Liu and X. Wang, Unique Starch Polymer Electrolyte for High Capacity All-Solid-State Lithium Sulfur Battery, *Green Chem.*, 2016, **18**(13), 3796–3803, DOI: 10.1039/C6GC00444J.
11 Y. Cui, J. Wan, Y. Ye, K. Liu, L.-Y. Chou and Y. Cui, A Fireproof, Lightweight, Polymer–Polymer Solid-State

Electrolyte for Safe Lithium Batteries, *Nano Lett.*, 2020, **20**(3), 1686–1692, DOI: 10.1021/acs.nanolett.9b04815.

12 S. Xu and L. Ye, Preparation and Properties of Monomer Casting Nylon-6/PEO Blend Prepared via *in Situ* Polymerization, *Polym. Eng. Sci.*, 2015, **55**(3), 589–597, DOI: 10.1002/pen.23923.

13 H. T. Ahmed and O. G. Abdullah, Preparation and Composition Optimization of PEO:MC Polymer Blend Films to Enhance Electrical Conductivity, *Polymers*, 2019, **11**(5), 853, DOI: 10.3390/polym11050853.

14 R. Bakar, S. Darvishi, T. Li, M. Han, U. Aydemir, S. Nizamoglu, K. Hong and E. Senses, Effect of Polymer Topology on Microstructure, Segmental Dynamics, and Ionic Conductivity in PEO/PMMA-Based Solid Polymer Electrolytes, *ACS Appl. Polym. Mater.*, 2022, **4**(1), 179–190, DOI: 10.1021/acsapm.1c01178.

15 N. A. Stolwijk, M. Wiencierz, C. Heddier and J. Kösters, What Can We Learn from Ionic Conductivity Measurements in Polymer Electrolytes? A Case Study on Poly(Ethylene Oxide) (PEO)–NaI and PEO–LiTFSI, *J. Phys. Chem. B*, 2012, **116**(10), 3065–3074, DOI: 10.1021/jp2111956.

16 K. I. S. Mongcopa, M. Tyagi, J. P. Mailoa, G. Samsonidze, B. Kozinsky, S. A. Mullin, D. A. Gribble, H. Watanabe and N. P. Balsara, Relationship between Segmental Dynamics Measured by Quasi-Elastic Neutron Scattering and Conductivity in Polymer Electrolytes, *ACS Macro Lett.*, 2018, **7**(4), 504–508, DOI: 10.1021/acsmacrolett.8b00159.

17 D. Devaux, R. Bouchet, D. Glé and R. Denoyel, Mechanism of Ion Transport in PEO/LiTFSI Complexes: Effect of Temperature, Molecular Weight and End Groups, *Solid State Ion.*, 2012, **227**, 119–127, DOI: 10.1016/j.ssi.2012.09.020.

18 J.-C. Wang, W.-J. Zhou, N. Zhang, P.-F. Wang and T.-F. Yi, Review on Poly(Ethylene Oxide)-Based Solid Electrolytes: Key Issues, Potential Solutions, and Outlook, *Energy Fuels*, 2024, **38**(19), 18395–18412, DOI: 10.1021/acs.energyfuels.4c03846.

19 Z. Xue, D. He and X. Xie, Poly(Ethylene Oxide)-Based Electrolytes for Lithium-Ion Batteries, *J. Mater. Chem. A*, 2015, **3**(38), 19218–19253, DOI: 10.1039/C5TA03471J.

20 C. Li, P. Xue, L. Chen, J. Liu and Z. Wang, Reducing the Crystallinity of PEO-Based Composite Electrolyte for High Performance Lithium Batteries, *Compos. Part B Eng.*, 2022, **234**, 109729, DOI: 10.1016/j.compositesb.2022.109729.

21 Y. Zheng, Y. Yao, J. Ou, M. Li, D. Luo, H. Dou, Z. Li, K. Amine, A. Yu and Z. Chen, A Review of Composite Solid-State Electrolytes for Lithium Batteries: Fundamentals, Key Materials and Advanced Structures, *Chem. Soc. Rev.*, 2020, **49**(23), 8790–8839, DOI: 10.1039/D0CS00305K.

22 Z. Stoeva, I. Martin-Litas, E. Staunton, Y. G. Andreev and P. G. Bruce, Ionic Conductivity in the Crystalline Polymer Electrolytes PEO_6: $LiXF_6$, X = P, As, Sb, *J. Am. Chem. Soc.*, 2003, **125**(15), 4619–4626, DOI: 10.1021/ja029326t.

23 X. Yang, M. Jiang, X. Gao, D. Bao, Q. Sun, N. Holmes, H. Duan, S. Mukherjee, K. Adair, C. Zhao, J. Liang, W. Li, J. Li, Y. Liu, H. Huang, L. Zhang, S. Lu, Q. Lu, R. Li, C. V. Singh and X. Sun, Determining the Limiting Factor of the Electrochemical Stability Window for PEO-Based Solid Polymer Electrolytes: Main Chain or Terminal –OH Group?, *Energy Environ. Sci.*, 2020, **13**(5), 1318–1325, DOI: 10.1039/D0EE00342E.

24 X. Wu and J. F. Whitacre, Reevaluating the Stability of the PEO-Based Solid-State Electrolytes for High Voltage Solid-State Batteries, *J. Energy Storage*, 2023, **63**, 107052, DOI: 10.1016/j.est.2023.107052.

25 J. Qiu, X. Liu, R. Chen, Q. Li, Y. Wang, P. Chen, L. Gan, S. Lee, D. Nordlund, Y. Liu, X. Yu, X. Bai, H. Li and L. Chen, Enabling Stable Cycling of 4.2 V High–Voltage All–Solid–State Batteries with PEO–Based Solid Electrolyte, *Adv. Funct. Mater.*, 2020, **30**(22), 1909392, DOI: 10.1002/adfm.201909392.

26 D. Zhang, L. Li, X. Wu, J. Wang, Q. Li, K. Pan and J. He, Research Progress and Application of PEO-Based Solid State Polymer Composite Electrolytes, *Front. Energy Res.*, 2021, **9**, 726738, DOI: 10.3389/fenrg.2021.726738.

27 J. Feng, L. Wang, Y. Chen, P. Wang, H. Zhang and X. He, PEO Based Polymer-Ceramic Hybrid Solid Electrolytes: A Review, *Nano Converg.*, 2021, **8**(1), 2, DOI: 10.1186/s40580-020-00252-5.

28 X. Liu, W. Mao, J. Gong, H. Liu, Y. Shao, L. Sun, H. Wang and C. Wang, Enhanced Electrochemical Performance of PEO-Based Composite Polymer Electrolyte with Single-Ion Conducting Polymer Grafted SiO_2 Nanoparticles, *Polymers*, 2023, **15**(2), 394, DOI: 10.3390/polym15020394.

29 P. Ghorbanzade, G. Accardo, K. Gomez, P. López-Aranguren, S. Devaraj, C. M. Costa, S. Lanceros-Mendez and J. M. López Del Amo, Influence of the LLZO–PEO Interface on the Micro- and Macro-Scale Properties of Composite Polymer Electrolytes for Solid-State Batteries, *Mater. Today Energy*, 2023, **38**, 101448, DOI: 10.1016/j.mtener.2023.101448.

30 F. Ma, Y. Liu, X. Du and Q. Lu, Hybrid Solid Electrolyte with the Combination of LATP Ceramic and PEO Polymer by a Solvent-Free Procedure, *Solid State Ion.*, 2024, **405**, 116450, DOI: 10.1016/j.ssi.2023.116450.

31 Y. Kumar, S. A. Hashmi and G. P. Pandey, Lithium Ion Transport and Ion–Polymer Interaction in PEO Based Polymer Electrolyte Plasticized with Ionic Liquid, *Solid State Ion.*, 2011, **201**(1), 73–80, DOI: 10.1016/j.ssi.2011.08.010.

32 A. Boschin and P. Johansson, Plasticization of NaX-PEO Solid Polymer Electrolytes by Pyr13X Ionic Liquids, *Electrochim. Acta*, 2016, **211**, 1006–1015, DOI: 10.1016/j.electacta.2016.06.119.

33 G. Campos-Villalobos, F. R. Siperstein, A. Charles and A. Patti, Solvent-Induced Morphological Transitions in Methacrylate-Based Block-Copolymer Aggregates, *J. Colloid Interface Sci.*, 2020, **572**, 133–140, DOI: 10.1016/j.jcis.2020.03.067.

34 D. Daubian, A. Fillion, J. Gaitzsch and W. Meier, One-Pot Synthesis of an Amphiphilic ABC Triblock Copolymer

PEO- *b* -PEHOx- *b* -PEtOz and Its Self-Assembly into Nanoscopic Asymmetric Polymersomes, *Macromolecules*, 2020, **53**(24), 11040–11050, DOI: 10.1021/acs.macromol.0c02301.

35 M. F. J. Mabesoone, J. D. Gopez, I. E. Paulus and D. Klinger, Tunable Biohybrid Hydrogels from Coacervation of Hyaluronic Acid and PEO–based Block Copolymers, *J. Polym. Sci.*, 2020, **58**(9), 1276–1287, DOI: 10.1002/pol.20200081.

36 F. Wu, L. Luo, Z. Tang, D. Liu, Z. Shen and X.-H. Fan, Block Copolymer Electrolytes with Excellent Properties in a Wide Temperature Range, *ACS Appl. Energy Mater.*, 2020, **3**(7), 6536–6543, DOI: 10.1021/acsaem.0c00737.

37 S. Li, M. Tian, J. Wang, F. Du, L. Li and Z. Xue, Poly (Ethylene Oxide)-Based Block Copolymer Electrolytes Formed via Ligand-Free Iron-Mediated Atom Transfer Radical Polymerization, *Polymers*, 2020, **12**(4), 763, DOI: 10.3390/polym12040763.

38 L. Kunitskaya, T. Zheltonozhskaya, S. Nesin and V. Klepko, Polymer Electrolyte Membranes Based on PEO-Containing Block Copolymers, *Mol. Cryst. Liq. Cryst.*, 2021, **717**(1), 136–142, DOI: 10.1080/15421406.2020.1862456.

39 D. Sharon, P. Bennington, M. A. Webb, C. Deng, J. J. De Pablo, S. N. Patel and P. F. Nealey, Molecular Level Differences in Ionic Solvation and Transport Behavior in Ethylene Oxide-Based Homopolymer and Block Copolymer Electrolytes, *J. Am. Chem. Soc.*, 2021, **143**(8), 3180–3190, DOI: 10.1021/jacs.0c12538.

40 L. Yang, Y. Nie, Y. Liu, Y. Zheng, D. Luo, N. Yang, Q. Ma, M. Xu, X. Ma, A. Yu, L. Shui, X. Wang and Z. Chen, The Plasticizer-Free Composite Block Copolymer Electrolytes for Ultralong Lifespan All-Solid-State Lithium-Metal Batteries, *Nano Energy*, 2022, **100**, 107499, DOI: 10.1016/j.nanoen.2022.107499.

41 Z.-K. Zhang, S.-P. Ding, Z. Ye, D.-L. Xia and J.-T. Xu, PEO-Based Block Copolymer Electrolytes Containing Double Conductive Phases with Improved Mechanical and Electrochemical Properties, *Materials*, 2022, **15**(22), 7930, DOI: 10.3390/ma15227930.

42 Masud, H. Zhou and H. K. Kim, Minimization of Photovoltage Loss of Iodine Electrolytes by Ethylene Carbonate and PAN-Based Block Copolymer for High-Performance Quasi-Solid-State Organic Dye-Sensitized Solar Cells, *ACS Appl. Polym. Mater.*, 2023, **5**(11), 9671–9680, DOI: 10.1021/acsapm.3c02272.

43 N. Tripathi, D. Ray, V. K. Aswal, K. Kuperkar and P. Bahadur, Salt Induced Micellization Conduct in PEO–PPO–PEO-Based Block Copolymers: A Thermo-Responsive Approach, *Soft Matter*, 2023, **19**(37), 7227–7244, DOI: 10.1039/D3SM00896G.

44 P. J. Das, V. Kumawat, M. Singla, M. R. Singh and S. Chandra Mohapatra, Self-Aggregation, Behavior of Well-Defined PEO-Based Amphiphilic Tri-Block Copolymers and Their Application as Metal Detectors, *J. Macromol. Sci., Part A*, 2024, **61**(12), 1085–1094, DOI: 10.1080/10601325.2024.2431933.

45 D. Wu, F. Xu, Y. Huang, C. Chen, C. Yu, X. Feng, D. Yan and Y. Mai, Effect of Side Chains on the Low-Dimensional Self-Assembly of Polyphenylene-Based "Rod–Coil" Graft Copolymers in Solution, *Macromolecules*, 2018, **51**(1), 161–172, DOI: 10.1021/acs.macromol.7b02002.

46 Y. He, Y. Yang, X. Ji, Q. Zhang, T. Jiang, H. Shi, S. Luan, R. K. Y. Li and D. Shi, Preparation of Polymer Electrolyte Membranes with Continuous PEG Channel via the Fusion of Self-Assembled Polycyclooctene-Graft-Polyethylene Glycol Copolymer Micelles, *J. Membr. Sci.*, 2019, **572**, 358–364, DOI: 10.1016/j.memsci.2018.11.032.

47 D. A. Kang, K. Kim, S. S. Karade, H. Kim and J. Hak Kim, High-Performance, Solid-State Bendable Supercapacitors Based on PEGBEM-g-PAEMA Graft Copolymer Electrolyte, *Chem. Eng. J.*, 2020, **384**, 123308, DOI: 10.1016/j.cej.2019.123308.

48 X. Ji, M. Cao, X. Fu, R. Liang, A. N. Le, Q. Zhang and M. Zhong, Efficient Room-Temperature Solid-State Lithium Ion Conductors Enabled by Mixed-Graft Block Copolymer Architectures, *Giant*, 2020, **3**, 100027, DOI: 10.1016/j.giant.2020.100027.

49 Y. Du, Y. Du, S. Lazzari, T. Reimers, R. Konradi, T. W. Holcombe and E. B. Coughlin, Mechanistic Investigation of Cyclic Ketene Acetal Radical Ring-Opening Homo- and Co-Polymerization and Preparation of PEO Graft Copolymers with Tunable Composition, *Polym. Chem.*, 2022, **13**(41), 5829–5840, DOI: 10.1039/D2PY00986B.

50 K. Guo, S. Li, Z. Shi, X. Zhou and Z. Xue, One–Step Polymerizations Enable Facile Construction and Structural Optimization of Graft Copolymer Electrolytes, *Macromol. Chem. Phys.*, 2023, **224**(24), 2300216, DOI: 10.1002/macp.202300216.

51 Q. Yang, J. Guo, S. Zhang, F. Guan, Y. Yu, Q. Yao, X. Zhang and Y. Xu, A Novel Biomedical Compatibilizer (Polyvinyl Alcohol–allyl Polyethylene Glycol Graft Copolymer) for Polyvinyl Alcohol/Polyethylene Oxide Composite System, *J. Appl. Polym. Sci.*, 2022, **139**(43), e53067, DOI: 10.1002/app.53067.

52 K. H. Khan, Y. Golitsyn, D. Reichert, J. Kressler and H. Hussain, Graphene Oxide-Grafted Hybrid Diblock Copolymer Brush (GO- *Graft* -PEG_{6k} - *Block* -P(MA-POSS)) as Nanofillers for Enhanced Lithium Ion Conductivity of PEO-Based Nanocomposite Solid Polymer Electrolytes, *J. Phys. Chem. B*, 2023, **127**(9), 2066–2082, DOI: 10.1021/acs.jpcb.2c07699.

53 X. Liu, W. Mao, J. Gong, H. Liu, Y. Shao, L. Sun, H. Wang and C. Wang, Enhanced Electrochemical Performance of PEO-Based Composite Polymer Electrolyte with Single-Ion Conducting Polymer Grafted SiO_2 Nanoparticles, *Polymers*, 2023, **15**(2), 394, DOI: 10.3390/polym15020394.

54 M. Falco, C. Simari, C. Ferrara, J. R. Nair, G. Meligrana, F. Bella, I. Nicotera, P. Mustarelli, M. Winter and C. Gerbaldi, Understanding the Effect of UV-Induced Cross-Linking on the Physicochemical Properties of Highly Performing PEO/LiTFSI-Based Polymer

Electrolytes, *Langmuir*, 2019, **35**(25), 8210–8219, DOI: 10.1021/acs.langmuir.9b00041.

55 Y. Zhang, W. Lu, L. Cong, J. Liu, L. Sun, A. Mauger, C. M. Julien, H. Xie and J. Liu, Cross-Linking Network Based on Poly(Ethylene Oxide): Solid Polymer Electrolyte for Room Temperature Lithium Battery, *J. Power Sources*, 2019, **420**, 63–72, DOI: 10.1016/j.jpowsour.2019.02.090.

56 I. Hossain, D. Kim, A. Z. Al Munsur, J. M. Roh, H. B. Park and T.-H. Kim, PEG/PPG–PDMS-Based Cross-Linked Copolymer Membranes Prepared by ROMP and In Situ Membrane Casting for CO_2 Separation: An Approach to Endow Rubbery Materials with Properties of Rigid Polymers, *ACS Appl. Mater. Interfaces*, 2020, **12**(24), 27286–27299, DOI: 10.1021/acsami.0c06926.

57 C. Zuo, G. Chen, Y. Zhang, H. Gan, S. Li, L. Yu, X. Zhou, X. Xie and Z. Xue, Poly(ε-Caprolactone)-Block-Poly(Ethylene Glycol)-Block-Poly(ε-Caprolactone)-Based Hybrid Polymer Electrolyte for Lithium Metal Batteries, *J. Membr. Sci.*, 2020, **607**, 118132, DOI: 10.1016/j.memsci.2020.118132.

58 L. Dong, X. Zeng, J. Fu, L. Chen, J. Zhou, S. Dai and L. Shi, Cross-Linked Ionic Copolymer Solid Electrolytes with Loose Coordination-Assisted Lithium Transport for Lithium Batteries, *Chem. Eng. J.*, 2021, **423**, 130209, DOI: 10.1016/j.cej.2021.130209.

59 P. Kianfar, A. Vitale, S. Dalle Vacche and R. Bongiovanni, Enhancing Properties and Water Resistance of PEO-Based Electrospun Nanofibrous Membranes by Photo-Crosslinking, *J. Mater. Sci.*, 2021, **56**(2), 1879–1896, DOI: 10.1007/s10853-020-05346-3.

60 J. Sheng, Q. Zhang, C. Sun, J. Wang, X. Zhong, B. Chen, C. Li, R. Gao, Z. Han and G. Zhou, Crosslinked Nanofiber–Reinforced Solid–State Electrolytes with Polysulfide Fixation Effect Towards High Safety Flexible Lithium–Sulfur Batteries, *Adv. Funct. Mater.*, 2022, **32**(40), 2203272, DOI: 10.1002/adfm.202203272.

61 F. Fu, Y. Zheng, N. Jiang, Y. Liu, C. Sun, A. Zhang, H. Teng, L. Sun and H. Xie, A Dual-Salt PEO-Based Polymer Electrolyte with Cross-Linked Polymer Network for High-Voltage Lithium Metal Batteries, *Chem. Eng. J.*, 2022, **450**, 137776, DOI: 10.1016/j.cej.2022.137776.

62 Y. Ji, Y.-H. Zhang, F.-N. Shi and L.-N. Zhang, UV-Derived, Double Crosslinked PEO-Based Solid Polymer Electrolyte for Room Temperature, *J. Colloid Interface Sci.*, 2023, **629**, 492–500, DOI: 10.1016/j.jcis.2022.09.089.

63 A. Naboulsi, R. Chometon, F. Ribot, G. Nguyen, O. Fichet and C. Laberty-Robert, Correlation between Ionic Conductivity and Mechanical Properties of Solid-like PEO-Based Polymer Electrolyte, *ACS Appl. Mater. Interfaces*, 2024, **16**(11), 13869–13881, DOI: 10.1021/acsami.3c19249.

64 G. Wang, X. Zhu, A. Rashid, Z. Hu, P. Sun, Q. Zhang and L. Zhang, Organic Polymeric Filler-Amorphized Poly (Ethylene Oxide) Electrolyte Enables All-Solid-State Lithium–Metal Batteries Operating at 35 °C, *J. Mater. Chem. A*, 2020, **8**(26), 13351–13363, DOI: 10.1039/D0TA00335B.

65 Z. Zeng, G. Liu, Z. Jiang, L. Peng and J. Xie, Zinc Bis (2−Ethylhexanoate), a Homogeneous and Bifunctional Additive, to Improve Conductivity and Lithium Deposition for Poly (Ethylene Oxide) Based All-Solid-State Lithium Metal Battery, *J. Power Sources*, 2020, **451**, 227730, DOI: 10.1016/j.jpowsour.2020.227730.

66 C.-C. Sun, A. Yusuf, S.-W. Li, X.-L. Qi, Y. Ma and D.-Y. Wang, Metal Organic Frameworks Enabled Rational Design of Multifunctional PEO-Based Solid Polymer Electrolytes, *Chem. Eng. J.*, 2021, **414**, 128702, DOI: 10.1016/j.cej.2021.128702.

67 C. H. Ahn, J. J. Kim, W. S. Yang and H. K. Cho, Multiple Functional Biomolecule-Based Metal-Organic-Framework-Reinforced Polyethylene Oxide Composite Electrolytes for High-Performance Solid-State Lithium Batteries, *J. Power Sources*, 2023, **557**, 232528, DOI: 10.1016/j.jpowsour.2022.232528.

68 H. Aziam, A. Ouarga, O. Ettalibi, D. Shanmukaraj, H. Noukrati, H. Sehaqui, I. Saadoune, A. Barroug and H. Ben Youcef, Phosphorylated, Cellulose Nanofiber as Sustainable Organic Filler and Potential Flame-Retardant for All-Solid-State Lithium Batteries, *J. Energy Storage*, 2023, **62**, 106838, DOI: 10.1016/j.est.2023.106838.

69 J. Chen and S. Han, PEO-Based Solid-State Electrolyte Modified by Cationic Covalent Organic Frameworks Enabling High-Performance All-Solid-State Li Metal and Graphite Anode Batteries, *Chem. Eng. J.*, 2023, **470**, 144150, DOI: 10.1016/j.cej.2023.144150.

70 L. Chen, Y. Li, S.-P. Li, L.-Z. Fan, C.-W. Nan and J. B. Goodenough, PEO/Garnet Composite Electrolytes for Solid-State Lithium Batteries: From "Ceramic-in-Polymer" to "Polymer-in-Ceramic", *Nano Energy*, 2018, **46**, 176–184, DOI: 10.1016/j.nanoen.2017.12.037.

71 L. Xu, J. Li, W. Deng, L. Li, G. Zou, H. Hou, L. Huang and X. Ji, Boosting the Ionic Conductivity of PEO Electrolytes by Waste Eggshell-Derived Fillers for High-Performance Solid Lithium/Sodium Batteries, *Mater. Chem. Front.*, 2021, **5**(3), 1315–1323, DOI: 10.1039/D0QM00541J.

72 Y.-W. Song, K. Heo, J. Lee, D. Hwang, M.-Y. Kim, S.-J. Kim, J. Kim and J. Lim, Lithium-Ion Transport in Inorganic Active Fillers Used in PEO-Based Composite Solid Electrolyte Sheets, *RSC Adv.*, 2021, **11**(51), 31855–31864, DOI: 10.1039/D1RA06210G.

73 B. Ramkumar, V. Aravindan, H. Ramasamy, K. V. Ajeya, J.-G. Ryu, H.-Y. Jung and Y.-S. Lee, Ternary Metal Oxide Filled PEO-Based Polymer Electrolyte for Solid-State Lithium Metal Battery: The Role of Filler Particle Size, *Solid State Sci.*, 2022, **132**, 106958, DOI: 10.1016/j.solidstatesciences.2022.106958.

74 J. Chen, X. Zheng, X. Wang, N. Fu and Z. Yang, Porous Inorganic Filler Li4.7Ag1.63GeS4.8 in PEO Electrolyte Effectively Inhibits Li Dendrites for All-Solid-State Li Metal Batteries, *Mater. Today Chem.*, 2023, **27**, 101321, DOI: 10.1016/j.mtchem.2022.101321.

75 N. Lv, Q. Zhang, Y. Xu, H. Li, Z. Wei, Z. Tao, Y. Wang and H. Tang, PEO-Based Composite Solid Electrolyte for

Lithium Battery with Enhanced Interface Structure, *J. Alloys Compd.*, 2023, **938**, 168675, DOI: 10.1016/j.jallcom.2022.168675.

76 M. Wang, L. Tian, Y. Cao, Z. Su, W. Zhang, S. Yi, Y. Zhang, B. Niu and D. Long, Surface Positive-Charged Modification of Inorganic Fillers to Optimize Lithium Ion Conductive Pathways in Composite Polymer Electrolytes for Lithium-Metal Batteries, *J. Colloid Interface Sci.*, 2023, **630**, 634–644, DOI: 10.1016/j.jcis.2022.10.137.

77 X. Yin, W. Feng, S. Cheng, Q. Huang, X. Zou, Z. Wang, X. Yang, S. Lu, X. Lu and Y. Zhao, Chemically Bonding Inorganic Fillers with Polymer to Achieve Ultra-Stable Solid-State Sodium Batteries, *J. Colloid Interface Sci.*, 2023, **648**, 855–864, DOI: 10.1016/j.jcis.2023.06.064.

78 D. Shang, J. Fu, Q. Lu, L. Chen, J. Yin, X. Dong, Y. Xu, R. Jia, S. Yuan, Y. Chen and W. Deng, A Novel Polyhedral Oligomeric Silsesquioxane Based Ionic Liquids (POSS-ILs) Polymer Electrolytes for Lithium Ion Batteries, *Solid State Ion.*, 2018, **319**, 247–255, DOI: 10.1016/j.ssi.2018.01.050.

79 Y. Li, Z. Sun, L. Shi, S. Lu, Z. Sun, Y. Shi, H. Wu, Y. Zhang and S. Ding, Poly(Ionic Liquid)-Polyethylene Oxide Semi-Interpenetrating Polymer Network Solid Electrolyte for Safe Lithium Metal Batteries, *Chem. Eng. J.*, 2019, **375**, 121925, DOI: 10.1016/j.cej.2019.121925.

80 J. Tan, X. Ao, A. Dai, Y. Yuan, H. Zhuo, H. Lu, L. Zhuang, Y. Ke, C. Su, X. Peng, B. Tian and J. Lu, Polycation Ionic Liquid Tailored PEO-Based Solid Polymer Electrolytes for High Temperature Lithium Metal Batteries, *Energy Storage Mater.*, 2020, **33**, 173–180, DOI: 10.1016/j.ensm.2020.08.009.

81 Z. Hu, X. Zhang and S. Chen, A Graphene Oxide and Ionic Liquid Assisted Anion-Immobilized Polymer Electrolyte with High Ionic Conductivity for Dendrite-Free Lithium Metal Batteries, *J. Power Sources*, 2020, **477**, 228754, DOI: 10.1016/j.jpowsour.2020.228754.

82 D. Cai, X. Wu, J. Xiang, M. Li, H. Su, X. Qi, X. Wang, X. Xia, C. Gu and J. Tu, Ionic-Liquid-Containing Polymer Interlayer Modified PEO-Based Electrolyte for Stable High-Voltage Solid-State Lithium Metal Battery, *Chem. Eng. J.*, 2021, **424**, 130522, DOI: 10.1016/j.cej.2021.130522.

83 Z. Lei, J. Shen, J. Wang, Q. Qiu, G. Zhang, S.-S. Chi, H. Xu, S. Li, W. Zhang, Y. Zhao, Y. Deng and C. Wang, Composite Polymer Electrolytes with Uniform Distribution of Ionic Liquid-Grafted ZIF-90 Nanofillers for High-Performance Solid-State Li Batteries, *Chem. Eng. J.*, 2021, **412**, 128733, DOI: 10.1016/j.cej.2021.128733.

84 A. R. Polu, A. A. Kareem and H. K. Rasheed, Thermal, Electrical and Electrochemical Properties of Ionic Liquid-Doped Poly(Ethylene Oxide)–LiTDI Polymer Electrolytes for Li-Ion Batteries, *J. Solid State Electrochem.*, 2023, **27**(2), 409–416, DOI: 10.1007/s10008-022-05333-5.

85 M. Zhang, F. Makhlooghiazad, U. Pal, M. Maleki, S. Kondou, G. A. Elia, C. Gerbaldi and M. Forsyth, Synergistic Combination of Cross-Linked Polymer and Concentrated Ionic Liquid for Electrolytes with High Stability in Solid-State Lithium Metal Batteries, *ACS Appl. Polym. Mater.*, 2024, **6**(23), 14469–14476, DOI: 10.1021/acsapm.4c02520.

86 X. Zhu, Z. Fang, Q. Deng, Y. Zhou, X. Fu, L. Wu, W. Yan and Y. Yang, Poly(Ionic Liquid)@PEGMA Block Polymer Initiated Microphase Separation Architecture in Poly(Ethylene Oxide)-Based Solid-State Polymer Electrolyte for Flexible and Self-Healing Lithium Batteries, *ACS Sustainable Chem. Eng.*, 2022, **10**(13), 4173–4185, DOI: 10.1021/acssuschemeng.1c08306.

87 R. K. Arya and A. K. Gupta, The Effect of Nitrogen-Rich Ionic Liquid [EMIMDCA] on the Electronic Structure of Solid Polymer Electrolyte (PEO-LiTFSI), *J. Mol. Model.*, 2022, **28**(11), 363, DOI: 10.1007/s00894-022-05353-y.

88 H. Yuan, J. Luan, Z. Yang, J. Zhang, Y. Wu, Z. Lu and H. Liu, Single Lithium-Ion Conducting Solid Polymer Electrolyte with Superior Electrochemical Stability and Interfacial Compatibility for Solid-State Lithium Metal Batteries, *ACS Appl. Mater. Interfaces*, 2020, **12**(6), 7249–7256, DOI: 10.1021/acsami.9b20436.

89 M. Martinez-Ibañez, E. Sanchez–Diez, L. Qiao, Y. Zhang, X. Judez, A. Santiago, I. Aldalur, J. Carrasco, H. Zhu, M. Forsyth, M. Armand and H. Zhang, Unprecedented Improvement of Single Li–Ion Conductive Solid Polymer Electrolyte Through Salt Additive, *Adv. Funct. Mater.*, 2020, **30**(16), 2000455, DOI: 10.1002/adfm.202000455.

90 H. Li, Y. Du, Q. Zhang, Y. Zhao and F. Lian, A Single–Ion Conducting Network as Rationally Coordinating Polymer Electrolyte for Solid–State Li Metal Batteries, *Adv. Energy Mater.*, 2022, **12**(13), 2103530, DOI: 10.1002/aenm.202103530.

91 F. Lu, G. Li, Y. Yu, X. Gao, L. Zheng and Z. Chen, Zwitterionic Impetus on Single Lithium-Ion Conduction in Solid Polymer Electrolyte for All-Solid-State Lithium-Ion Batteries, *Chem. Eng. J.*, 2020, **384**, 123237, DOI: 10.1016/j.cej.2019.123237.

92 Y. Zhao, Y. Bai, Y. Bai, M. An, G. Chen, W. Li, C. Li and Y. Zhou, A Rational Design of Solid Polymer Electrolyte with High Salt Concentration for Lithium Battery, *J. Power Sources*, 2018, **407**, 23–30, DOI: 10.1016/j.jpowsour.2018.10.045.

93 J. Zhang, Y. Zeng, Q. Li, Z. Tang, D. Sun, D. Huang, L. Zhao, Y. Tang and H. Wang, Polymer-in-Salt Electrolyte Enables Ultrahigh Ionic Conductivity for Advanced Solid-State Lithium Metal Batteries, *Energy Storage Mater.*, 2023, **54**, 440–449, DOI: 10.1016/j.ensm.2022.10.055.

94 S. Li, Y.-M. Chen, W. Liang, Y. Shao, K. Liu, Z. Nikolov and Y. Zhu, A Superionic Conductive, Electrochemically Stable Dual-Salt Polymer Electrolyte, *Joule*, 2018, **2**(9), 1838–1856, DOI: 10.1016/j.joule.2018.06.008.

95 J. Yu, J. Liu, X. Lin, H. M. Law, G. Zhou, S. C. T. Kwok, M. J. Robson, J. Wu and F. Ciucci, A Solid-like Dual-Salt Polymer Electrolyte for Li-Metal Batteries Capable of Stable Operation over an Extended Temperature Range, *Energy Storage Mater.*, 2021, **37**, 609–618, DOI: 10.1016/j.ensm.2021.02.045.

96 H. C. Lee, M. Kim, M. Kim, T. W. Yoon, M. Kim, H. S. Lee, D. S. Ham, D. Lee, C. Ha, Y. Kim and B. Kang, Dual–

Supporter and Dual–Salt Strategy for Solid Polymer Electrolyte with High Ionic Conductivity and Elastic Toughness, *Adv. Electron. Mater.*, 2023, **9**(8), 2300094, DOI: 10.1002/aelm.202300094.

97 Y. Cui, J. Wan, Y. Ye, K. Liu, L.-Y. Chou and Y. Cui, A Fireproof, Lightweight, Polymer–Polymer Solid-State Electrolyte for Safe Lithium Batteries, *Nano Lett.*, 2020, **20**(3), 1686–1692, DOI: 10.1021/acs.nanolett.9b04815.

98 X. Liu, C. Zhang, S. Gao, S. Cai, Q. Wang, J. Liu and Z. Liu, A Novel Polyphosphonate Flame-Retardant Additive towards Safety-Reinforced All-Solid-State Polymer Electrolyte, *Mater. Chem. Phys.*, 2020, **239**, 122014, DOI: 10.1016/j.matchemphys.2019.122014.

99 J. L. Olmedo-Martínez, L. Meabe, R. Riva, G. Guzmán-González, L. Porcarelli, M. Forsyth, A. Mugica, I. Calafel, A. J. Müller, P. Lecomte, C. Jérôme and D. Mecerreyes, Flame Retardant Polyphosphoester Copolymers as Solid Polymer Electrolyte for Lithium Batteries, *Polym. Chem.*, 2021, **12**(23), 3441–3450, DOI: 10.1039/D1PY00344E.

100 L. Han, C. Liao, X. Mu, N. Wu, Z. Xu, J. Wang, L. Song, Y. Kan and Y. Hu, Flame-Retardant ADP/PEO Solid Polymer Electrolyte for Dendrite-Free and Long-Life Lithium Battery by Generating Al, P-Rich SEI Layer, *Nano Lett.*, 2021, **21**(10), 4447–4453, DOI: 10.1021/acs.nanolett.1c01137.

101 Y. Chen, Y. Wang, Z. Li, D. Wang, H. Yuan, H. Zhang and Y. Tan, A Flame Retarded Polymer-Based Composite Solid Electrolyte Improved by Natural Polysaccharides, *Compos. Commun.*, 2021, **26**, 100774, DOI: 10.1016/j.coco.2021.100774.

102 X. Zheng, J. Wu, J. Chen, X. Wang and Z. Yang, 3D Flame-Retardant Skeleton Reinforced Polymer Electrolyte for Solid-State Dendrite-Free Lithium Metal Batteries, *J. Energy Chem.*, 2022, **71**, 174–181, DOI: 10.1016/j.jechem.2022.03.010.

103 N. Zhao, Y. Zou, X. Chen, H. Weng, C. Wang, Y. Zhu and Y. Mei, Enhanced Safety of Polymer Solid Electrolytes by Using Black Phosphorene as a Flame-Retardant, *Colloids Surf., A*, 2023, **666**, 131317, DOI: 10.1016/j.colsurfa.2023.131317.

104 Y. Liu, L. Han, C. Liao, H. Yu, Y. Kan and Y. Hu, Ultra-Thin, Non-Combustible PEO Polymer Solid Electrolyte for High Safety Polymer Lithium Metal Batteries, *Chem. Eng. J.*, 2023, **468**, 143222, DOI: 10.1016/j.cej.2023.143222.

105 X. Meng, X. Yang and X. Sun, Emerging Applications of Atomic Layer Deposition for Lithium–Ion Battery Studies, *Adv. Mater.*, 2012, **24**(27), 3589–3615, DOI: 10.1002/adma.201200397.

106 X. Meng, An Overview of Molecular Layer Deposition for Organic and Organic–Inorganic Hybrid Materials: Mechanisms, Growth Characteristics, and Promising Applications, *J. Mater. Chem. A*, 2017, **5**(35), 18326–18378, DOI: 10.1039/C7TA04449F.

107 Z. Song, H. Shi, F. Tian, J. Wang, Y. Liang, L. Xiang, X. Li and Z. Xu, Operando SAXS/WAXS Unveils Solvated Structure Dynamics in PVDF-Co-HFP Solid-State Electrolytes, *Nano Energy*, 2025, **142**, 111268, DOI: 10.1016/j.nanoen.2025.111268.

108 C. Liu, X. Tang, Y. Wang, R. L. Sacci, W. Bras, J. K. Keum and X. C. Chen, Ionic Conductivity Enhancement of Polymer Electrolytes by Directed Crystallization, *ACS Macro Lett.*, 2022, **11**(4), 595–602, DOI: 10.1021/acsmacrolett.2c00040.

109 Y. Ma, Q. Sun, S. Wang, Y. Zhou, D. Song, H. Zhang, X. Shi and L. Zhang, Li Salt Initiated *In situ* Polymerized Solid Polymer Electrolyte: New Insights via *in situ* Electrochemical Impedance Spectroscopy, *Chem. Eng. J.*, 2022, **429**, 132483, DOI: 10.1016/j.cej.2021.132483.

110 X. He, J. M. Larson, H. A. Bechtel and R. Kostecki, In Situ Infrared Nanospectroscopy of the Local Processes at the Li/Polymer Electrolyte Interface, *Nat. Commun.*, 2022, **13**(1), 1398, DOI: 10.1038/s41467-022-29103-z.

111 H. Cheng, C. B. Zhu, M. Lu and Y. Yang, In Situ Micro-FTIR Study of the Solid–Solid Interface between Lithium Electrode and Polymer Electrolytes, *J. Power Sources*, 2007, **174**(2), 1027–1031, DOI: 10.1016/j.jpowsour.2007.06.213.